1993-06

Effects of thrust vector control on the performance of the aerobang orbital plane change maneuver

Johnson, Richard E.

Monterey, California. Naval Postgraduate School

NAVAL POSTGRADUATE SCHOOL
Monterey, California

THESIS

EFFECTS OF THRUST VECTOR CONTROL
ON THE PERFORMANCE OF THE
AEROBANG ORBITAL PLANE
CHANGE MANEUVER

by

Richard E. Johnson

June 1993

Thesis Advisor: I. Michael Ross

REPORT DOCUMENTATION PAGE

1a Report Security Classification: Unclassified	1b Restrictive Markings
2a Security Classification Authority	3 Distribution/Availability of Report
2b Declassification/Downgrading Schedule	Approved for public release; distribution is unlimited.
4 Performing Organization Report Number(s)	5 Monitoring Organization Report Number(s)
6a Name of Performing Organization: Naval Postgraduate School / 6b Office Symbol (if applicable) 31	7a Name of Monitoring Organization: Naval Postgraduate School
6c Address (city, state, and ZIP code): Monterey CA 93943-5000	7b Address (city, state, and ZIP code): Monterey CA 93943-5000
8a Name of Funding/Sponsoring Organization / 6b Office Symbol (if applicable)	9 Procurement Instrument Identification Number
Address (city, state, and ZIP code)	10 Source of Funding Numbers: Program Element No / Project No / Task No / Work Unit Accession No

11 Title (include security classification) EFFECTS OF THRUST VECTOR CONTROL ON THE PERFORMANCE OF THE AEROBANG ORBITAL PLANE CHANGE MANEUVER (UNCLASSIFIED)

12 Personal Author(s) Johnson, Richard E.

13a Type of Report	13b Time Covered From To	14 Date of Report (year, month, day)	15 Page Count
Master's Thesis		June 1993	76

16 Supplementary Notation The views expressed in this thesis are those of the author and do not reflect the official policy or position of the Department of Defense or the U.S. Government.

17 Cosati Codes			18 Subject Terms
Field	Group	Subgroup	Aerobang, Synergetic, Aero-assist, MRRV

19 Abstract

The aerobang maneuver, one of three types of aero-assisted orbital change methods, holds the possibility of reducing fuel consumption for orbital craft capable of atmospheric entry. It has previously been shown that different types of vehicles provide varying results over a constant heating rate trajectory. Further investigation into the optimization of the aerobang maneuver in this thesis includes the effect of using thrust vector control, the examination of the effects of increasing fuel mass fraction to increase orbital inclination changes, and the effects of that increase on both angle of attack and heating rate. The aerobang maneuver is shown to be capable of significant changes in orbital inclination in either a fixed heating rate or a fixed angle of attack mode for the Maneuverable Reentry Research Vehicle.

20 Distribution/Availability of Abstract	21 Abstract Security Classification
X unclassified/unlimited ___ same as report ___ DTIC users	Unclassified
22a Name of Responsible Individual: I. M. Ross	22b Telephone (include Area Code): (408) 656-2074 / 22c Office Symbol: AA/Ro

DD FORM 1473,84 MAR 83 APR edition may be used until exhausted
All other editions are obsolete

security classification of this page: Unclassified

Approved for public release; distribution is unlimited.

Effects Of Thrust Vector Control On The Performance Of The Aerobang Orbital Plane Change Maneuver

by

Richard E. Johnson
Lieutenant, United States Navy
B.S., United States Naval Academy, 1984

Submitted in partial fulfillment
of the requirements for the degree of

MASTER OF SCIENCE IN ASTRONAUTICAL ENGINEERING

from the

NAVAL POSTGRADUATE SCHOOL
June 1993

ABSTRACT

The aerobang maneuver, one of three types of aero-assisted orbital change methods, holds the possibility of reducing fuel consumption for orbital craft capable of atmospheric entry. It has been previously shown that different types of vehicles provide varying results over a constant heating rate trajectory. Further investigation into the optimization of the aerobang maneuver in this thesis includes the effects of using thrust vector control, the examination of the effects of increasing fuel mass fraction to increase orbital inclination changes, and the effects of that increase on both angle of attack and heating rate. The aerobang maneuver is shown to be capable of significant changes in orbital inclination in either a fixed heating rate or a fixed angle of attack mode for the Maneuverable Reentry Research Vehicle.

C.1

TABLE OF CONTENTS

LIST OF FIGURES

LIST OF VARIABLES

a	Acceleration of the flight vehicle.
A_R	Vehicle acceleration in the normal (radial) direction.
A_S	Vehicle acceleration in the tangential direction.
A_W	Vehicle acceleration in the binormal direction.
C_D	Coefficient of Drag.
C_L	Coefficient of Lift.
C_1	Zeroth order coefficient of binomial expansion for C_L.
C_2	First order coefficient for C_L.
C_3	Second order coefficient for C_L.
C_4	Zeroth order coefficient of binomial expansion for C_D.
C_5	First order coefficient for C_D.
C_6	Second order coefficient for C_D.
D	Drag on flight vehicle.
F	Sum of all forces on the flight vehicle.
$F_{x'}$	Forces on vehicle along x' axis in vehicle frame of reference.
$F_{y'}$	Forces on vehicle along y' axis in vehicle frame of reference.
$F_{z'}$	Forces on vehicle along z' axis in vehicle frame of reference.
g	Local gravity.
h	Angular momentum of orbiting vehicle.

i	Orbit inclination
k	Unit vector along Z axis of the inertial coordinate system.
k	Coefficient for heating rate formula.
L	Lift on flight vehicle.
m_a	Mass of the flight vehicle.
m	Power coefficient for velocity in heating rate formula.
n	Power coefficient for density in heating rate formula.
Q	Stagnation point heating rate of flight vehicle
r	Geocentric radius of flight vehicle.
r_s	Reference geocentric radius for atmospheric model.
S	Reference surface area of vehicle.
T	Thrust of flight vehicle.
V	Velocity of flight vehicle.
X,Y,Z	Cartesian coordinates for inertial reference frame.
x,y,z	Cartesian coordinates for rotating reference frame.
x',y',z'	Cartesian coordinates for vehicle reference frame.
α	Angle of Attack of flight vehicle.
β	Coefficient for scale height in atmospheric model.
γ	Flight path angle, referenced to local horizon.
ε	Thrust vector angle.
θ	Right ascension of spacecraft.
ρ	Density of the atmosphere.
ρ_o	Reference density of the atmosphere.

ρ_s	Reference density of the atmosphere for atmospheric model.
σ	Angle of bank of the flight vehicle.
ϕ	Declination of spacecraft.
ψ	Heading of flight vehicle based on angle from equatorial plane.
Ω	Angular velocity of the vehicle's orbit.

I. INTRODUCTION

A. BACKGROUND

Almost all orbiting spacecraft have the ability to correct and change their orbits, either within a given orbital plane or by transferring to other planes for better positioning depending on the purpose of the spacecraft. These maneuvers are performed using the spacecraft's propulsion and attitude control systems and are limited by the amount of fuel the spacecraft can carry onboard.

Executing a non-coplanar transfer requires more fuel than an orbital change within the original plane, such as increasing or decreasing orbital velocity to change orbital radius or altitude. In addition to velocity changes, a non-coplanar transfer requires a change in the direction of travel of the spacecraft. Missions requiring numerous plane changes are greatly limited by the fuel capacity of the spacecraft.

Since the early 1960's, the possibility of using aerodynamic forces as a means of controlling both velocity and direction of a spacecraft has been studied [Ref. 1]. With a properly designed spacecraft, the Earth's atmosphere (or that of any other planet) could be used to assist the propulsive force of the spacecraft. Such a spacecraft would need to be

able to use the lift forces generated to overcome the drag present to maintain flight and be constructed to withstand the surface heating effects that would occur within the atmosphere at near orbital speeds. Figure 1 shows a simple schematic drawing of what an aerodynamically assisted orbital transfer would entail.

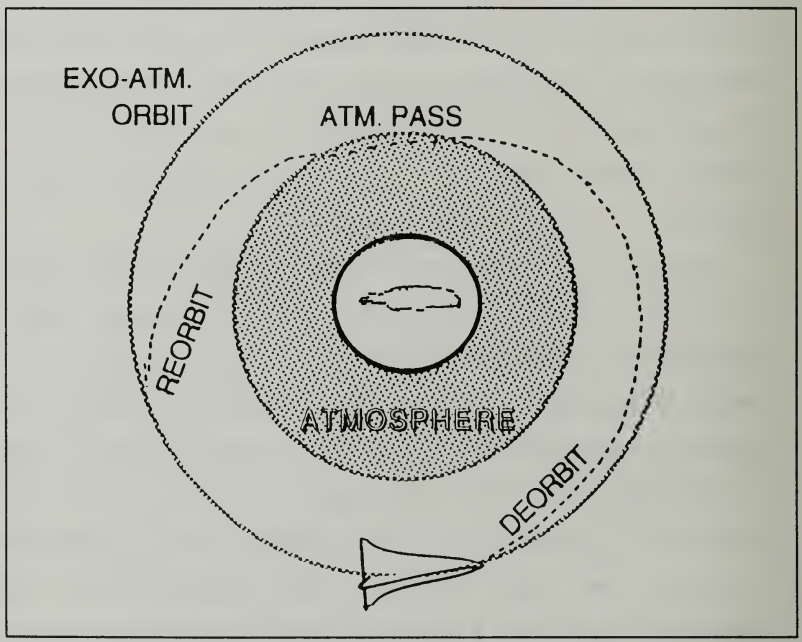

Figure 1 Aerodynamically Assisted Orbital Transfer

B. TYPES OF SYNERGETIC ORBITAL MANEUVERS

Synergetic maneuvers are defined as maneuvers that use both atmospheric (aerodynamic) and propulsive forces. For

orbital transfers between orbital planes, they have been divided into three categories: aeroglide, aerocruise, and aerobang.

1. Aeroglide

As the name implies, the aeroglide maneuver utilizes the aerodynamic forces present to create a gliding, unpowered trajectory. While fuel is required to deorbit prior to and reorbit after the maneuver, the aeroglide itself relies only on the lift generated by the spacecraft's interaction with the atmosphere. As a consequence of this, the glide must not only be performed at a sufficiently low altitude to take advantage of the more dense atmosphere, but also at velocities high enough to maintain flight. This results in extremely high surface heating rates, perhaps beyond the capacity of the spacecraft's structure to absorb or dissipate [Ref. 2]. This disadvantage makes the aeroglide maneuver less appealing for non-coplanar orbital transfers by itself, although it could conceivably be used in conjunction with another technique.

2. Aerocruise

The aerocruise maneuver uses the spacecraft's propulsive force as well as the aerodynamic forces present in a glide. The drag encountered by the spacecraft is exactly compensated for by the thrust generated by the spacecraft's engines. This allows the spacecraft to maintain a constant heating rate and avoid the overheating problems present with

the aeroglide. This requires both constant speed and altitude. The engine is throttled to maintain thrust sufficient to counteract drag, and the bank angle is adjusted to have a portion of the lift oppose the centrifugal force, thus maintaining a constant orbital radius or altitude. Changes in orbital inclination come as a result of the lift generated and will depend on the lift to drag ratio (L/D) and the angle of attack (α) of the vehicle. Altering these parameters will produce varying amounts of inclination change for a given amount of fuel burned.

3. Aerobang

This maneuver also uses a constant heating rate as a requirement, allowing the altitude and velocity to vary during the flight as dictated by the control law for the maneuver, discussed later. This allows a constant thrust to be used and allows the angle of attack to vary. The thrust is set at the maximum, reducing the time the spacecraft is in the atmosphere compared to the aerocruise, thus reducing the integrated heating effects on the spacecraft. It has previously been shown that, for certain velocities, altitudes, and heating rates, an aerobang maneuver will yield a greater orbital inclination change than an aerocruise maneuver, for the same fuel expenditure [Ref. 3].

C. SCOPE OF THESIS

This thesis will further examine the aerobang non-coplanar orbital transfer maneuver. The initial results showed that the maneuver generated smaller than expected inclination changes for the given two percent mass fraction of fuel consumed. The thrust acted in the direction of the spacecraft's body and thus only a portion (depending upon the angle of attack) acted to help the lift, which produced the inclination change. The effects of thrust vector control (TVC) are included here to allow the thrust to contribute further to the lift, and thus increase the inclination change while maintaining an angle of attack within the vehicle's capability.

The aerobang maneuver is limited by the amount of fuel allotted for each atmospheric pass. Obviously, the greater the fuel used, the longer the maneuver can be performed, subject to heating and altitude restraints. The initial results [Ref. 3] were based upon a 0.02 mass fraction because the aerobang maneuver was unable to maintain a constant heating rate profile beyond that point for some conditions of altitude and velocity. The inclination changes generated with this restriction (less than one degree for the most part) is not useful for many orbiting spacecraft applications. By expanding the allowable mass fraction of the fuel consumed for the maneuver to values up to twenty percent, larger, more useful inclination changes should be able to be produced.

In addition to the two limiting heating rates examined in Reference 3, the effects of both aerocruise and aerobang over the entire range of heating rates are studied. The intent is to determine the shape of the heating rate profile for both maneuvers and determine more precisely when aerobang is a superior method of orbital transfer. This study will also observe the behavior of the vehicle's angle of attack during extended constant heating rate maneuvers as well as fixing the angle of attack for other maneuvers and observing its effect on the heating rate.

D. FLIGHT VEHICLE

The vehicle used for this study is the Maneuverable Reentry Research Vehicle (MRRV). The MRRV was designed as a hypersonic research vehicle to be launched by the space shuttle and capable of a powered re-entry and flight through the atmosphere to demonstrate the feasibility of aerocruise maneuvers [Ref. 4]. The MRRV has also been used as a test vehicle for aerobang simulations [Ref. 3]. Because of this, and for consistency, it is used here as well.

As depicted in Figure 2 [Ref. 3], the MRRV is a winged body approximately 7.6 meters long with a four meter wingspan. The effective surface area is 11.61 m^2 with an initial mass of 4898 kg, of which 2588 kg is fuel. The MRRV is powered by

three Marquardt R-40-B rocket motors that provide a total thrust of 14679 Newtons with a specific impulse (I_{sp}) of 295 seconds.

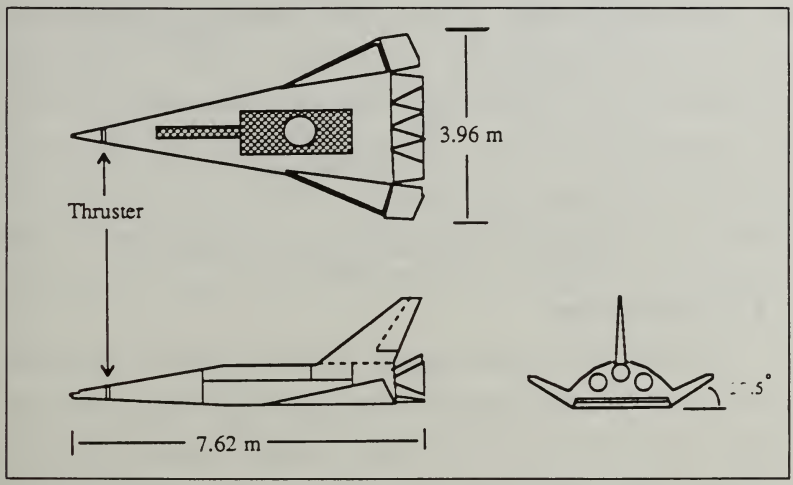

Figure 2 The MRRV

Figure 3 shows that the MRRV has a nominal lift to drag ratio (L/D) of 2.3 at its optimal angle of attack of 14 degrees. This is based upon wind tunnel data gathered out to an angle of attack of between 30 and 40 degrees [Ref. 4]. No data was available for higher values, implying that this is the upper limit for angle of attack for this vehicle.

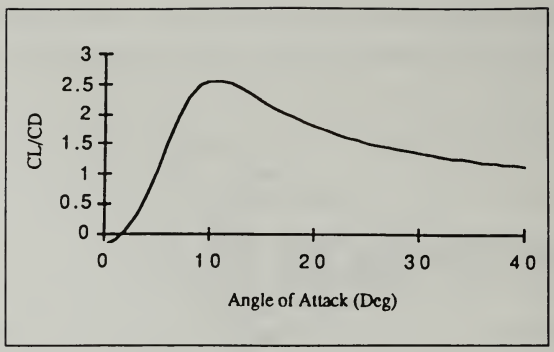

Figure 3 C_L/C_D and Angle of Attack for the MRRV

E. APPLICATIONS

Initially, it would appear that the results described in Reference 3 (and modified later in this thesis for the 2% case) may not be useful for most orbital transfer applications since they amount to less than a one degree change in inclination, occurring over a period of under 20 seconds. There are, however, possible applications and factors to take into account when studying these results.

An inclination change of even a degree or so can correspond to a difference of over a hundred kilometers when the angle is projected up to the orbital altitudes used here and higher as well. For example, for a one degree change in inclination at a radius of 6447 km, the spacecraft will move 112.5 km. In a military application involving pursued and pursuing vehicles in orbit, such as anti-satellite warfare, a quick aerobang maneuver resulting in even a small amount of

orbital transfer may be capable of preventing a vehicle from being detected or destroyed.

Even for civilian applications, a small aerobang maneuver may be preferred to a longer one to minimize the heat load imparted to a vehicle that may not have the thermal protection system to adequately protect against a longer atmospheric flight that would yield a greater inclination change. By making multiple, low fuel passes and reorbiting between orbital changes to radiate the heat to space, the same total inclination change can be made if time is not of the essence.

II. EQUATIONS OF MOTION

The motion of the aerodynamic spacecraft within its orbit is defined by six variables for both position and velocity. Position is defined by the standard spherical coordinates; r (radius), θ (right ascension), and ϕ (declination). The other three variables are v (velocity), γ (flight path angle), and ψ (heading angle). These variables are graphically shown in Figure 4 below.

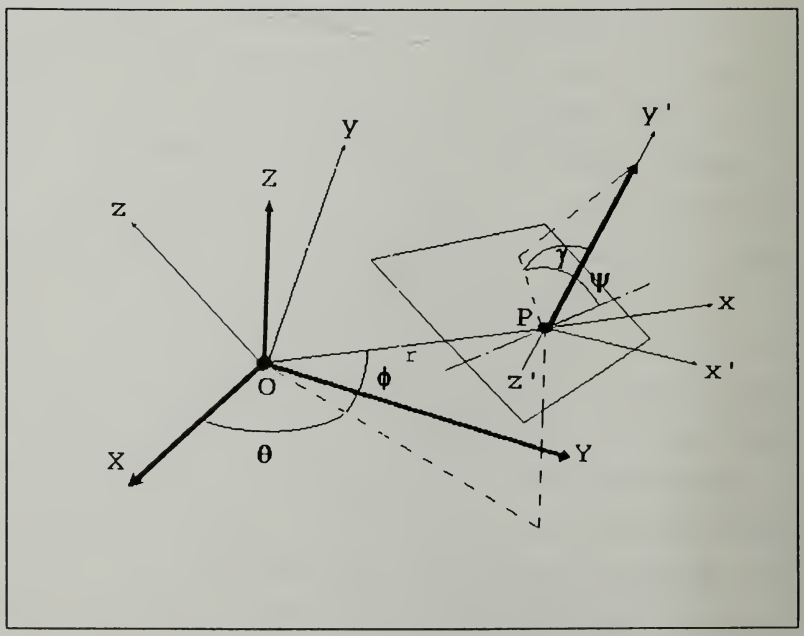

Figure 4 The Coordinate System

The flight path angle is described as the angle of the velocity vector with relation to the local horizontal plane tangent to the orbit and the heading angle is the direction angle within that plane relative to the local inertial latitude.These equations were derived [Ref. 3] assuming a spherical, non-rotating Earth. Atmospheric motion (winds) and the oblateness of the Earth were also neglected. The method of derivation and the resulting equations that were used in this study are summarized in this chapter.

A. SPACECRAFT POSITION

The derivation of the equations of motion requires the use of three coordinate systems. As shown in Figure 4, the position of the vehicle can be expressed in the inertial XYZ system, the orbital xyz system, also centered at the Earth's center, with the positive x axis pointed to the orbiting spacecraft, as well as the x'y'z' system which is centered on the spacecraft with the positive y' direction in line with the velocity vector and the x' axis within the xy plane.

Direction cosine matrices (DCM) are required to transform the various coordinate systems into one to be used for the expression of the spacecraft's position and velocity. In order to get from the inertial XYZ system to the orbital xyz system, a body 3-2 rotation through angles θ and ϕ is required. To obtain the xyz coordinates from the x'y'z' system a 3-1 rotation is used through angles γ and ψ.

By equating the velocity vector to the time derivative of the position vector for the spacecraft, the kinematics can be expressed as follows:

$$\frac{dr}{dt} = V\sin\gamma \tag{2.1}$$

$$\frac{d\theta}{dt} = \frac{V\cos\gamma\cos\psi}{r\cos\phi} \tag{2.2}$$

$$\frac{d\phi}{dt} = \frac{V\cos\gamma\sin\psi}{r} \tag{2.3}$$

The other three equations are based on the balance of forces on the spacecraft, and their relation to the accelerations and masses (F=ma). The forces are first derived in the spacecraft's frame of reference, the x'y'z' system, as shown in Figure 5.

The forces in the x', y' and z' directions are:

$$F_{x'} = [T\sin(\alpha+\epsilon)+L]\cos\sigma \tag{2.4}$$

$$F_{y'} = T\cos(\alpha+\epsilon)-D \tag{2.5}$$

$$F_{z'} = [T\sin(\alpha+\epsilon)]-D \tag{2.6}$$

Again, the conversion to the rotating reference, the xyz system, is done using the appropriate DCM. The resulting expressions for the forces on the spacecraft are then set

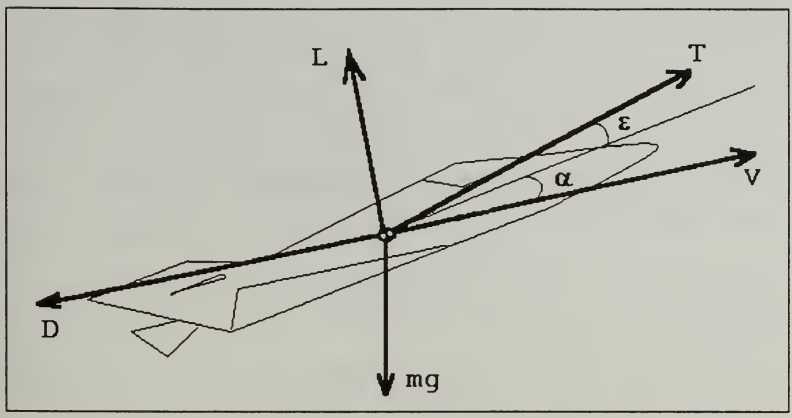

Figure 5 Spacecraft Force Diagram

equal to the product of the mass and the accelerations (calculated by taking the derivative of velocity vector) in each of the three direction components (x, y, and z) and are reduced to the following:

$$[T\cos(\alpha+\epsilon)-D]-m_a g\sin\gamma=m_a\frac{dV}{dt} \tag{2.7}$$

$$V\frac{d\gamma}{dt}=\frac{[T\sin(\alpha+\epsilon)+L]\cos\sigma-m_a g\cos\gamma}{m_a}+\frac{V^2}{r}\cos\gamma \tag{2.8}$$

$$V\frac{d\psi}{dt}=\frac{[T\sin(\alpha+\epsilon)+L]\sin\sigma}{m_a\cos\gamma}-\frac{V^2}{r}\cos\gamma\cos\psi\tan\phi \tag{2.9}$$

The components of the spacecraft's acceleration in the tangential, normal, and binormal directions can be expressed independently. This will allow the final three equations of

motion to be expressed in a more compact form. For a perfectly circular orbit, the normal (to the tangential velocity and acceleration vectors) direction is also the radial direction, pointing to the center of the Earth. Hence, the notation A_R for this component.

$$A_R = \frac{[T\sin(\alpha+\epsilon)+L]\cos\sigma}{m_a} \tag{2.10}$$

$$A_S = \frac{T\cos(\alpha+\epsilon)-D}{m_a} \tag{2.11}$$

$$A_W = \frac{[T\sin(\alpha+\epsilon)+L]\sin\sigma}{m_a} \tag{2.12}$$

The final three equations of motion then become:

$$\frac{dV}{dt} = A_S - g\sin\gamma \tag{2.13}$$

$$V\frac{d\gamma}{dt} = A_R + \left(\frac{V^2}{r} - g\right)\cos\gamma \tag{2.14}$$

$$V\frac{d\psi}{dt} = \frac{A_W}{\cos\gamma} + \frac{V^2}{r}\cos\gamma\cos\psi\tan\phi \tag{2.15}$$

B. ORBITAL INCLINATION

The measure of the effectiveness of the orbital plane change maneuver is the change in the orbit's inclination. Since the equations of motion use the spherical coordinates to describe the spacecraft's motion, the inclination must also be expressed in these coordinates. As shown in Reference 3, the

angular momentum vector will be perpendicular to the orbital plane so that the angle between that vector and the unit vector, **k**, defining the positive Z direction will be the orbit's inclination. The magnitude of the angular momentum vector is shown to be Vrcosγ while the Z component of the angular momentum is Vrcosγcosψ. Since

$$\vec{h}\cdot\vec{k}=|\vec{h}|\cos i \tag{2.16}$$

then

$$Vr\cos\gamma\cos\psi\cos\phi=|\vec{h}|\cos i \tag{2.17}$$

and so it follows that

$$\cos i=\cos\psi\cos\phi \tag{2.18}$$

giving a means of simply calculating the orbital inclination for any plane change maneuver.

III. HEATING RATE AND CONTROL LAWS

The control parameters for the aerobang maneuver are the bank angle, the angle of attack, and the thrust. The angle of bank is set to 90 degrees, the thrust is set to the maximum, and the angle of attack is adjusted to maintain a constant heating rate on the spacecraft during the maneuver. In order to implement a control law for the aerobang orbital transfer maneuver, the modeling of the atmosphere and resulting heating rate must first be developed.

A. ATMOSPHERIC MODEL

The first step in the modeling of the heating rate behavior is to model the atmosphere in the region in which the maneuvers will take place. For the aerobang maneuvers examined in this and previous studies, the region between the altitudes of 50 and 120 km was used. The density of the air at these altitudes was modeled using the U.S. Standard Atmosphere, 1976, [Ref. 5, p. 7] and is approximated by a local exponential model

$$\rho = \rho_s e^{-\beta(r-r_s)} \tag{3.1}$$

where

$$\rho_s = 3.0968 \times 10^{-4} \text{ kg/m}^3$$

$$\beta = 1.41\times10^{-4}\ m^{-1}$$

$$r_s = 6438\ km$$

B. HEATING RATE MODEL

Atmospheric density (and therefore altitude, as shown above) along with the vehicle's velocity combine to give a basic relationship for the heating rate. As shown in Reference 5, that relationship is:

$$\dot{Q}=k\rho^{n}V^{m} \tag{3.2}$$

with k, n, and m as constants. This equation, combined with the equations of motion can be used to derive the angle of attack required to fly at a constant heating rate during the aerobang maneuver.

By combining Equations 3.1 and 3.2, the relationship between density, heating rate, and velocity becomes more apparent.

$$V=\left[\frac{\dot{Q}}{k\rho_o{}^{n}e^{-\beta(r-r_s)}}\right]^{\frac{1}{m}} \tag{3.3}$$

In order to show the effect of the heating rate model on the equations of motion, the derivative of Equation 3.3 is taken, and simplified to give:

$$\frac{dV}{dt}=\left[\frac{\beta n}{m}\right]V\frac{dr}{dt} \tag{3.4}$$

Using Equation 2.1, the expression for dr/dt can be used to express dV/dt as a function of V and γ, the flight path angle.

$$\frac{dV}{dt}=\left[\frac{\beta n}{m}\right]V^2\sin\gamma \qquad (3.5)$$

Using Equations 2.11 and 2.13 gives for the equation along the path,

$$\frac{dV}{dt}=\frac{T\cos(\alpha+\epsilon)-D}{m_a}-g\sin\gamma \qquad (3.6)$$

C. DETERMINING THE ANGLE OF ATTACK

Equating Equations 3.5 and 3.6 gives an expression for calculating the angle of attack required for the aerobang maneuver:

$$0=T\cos(\alpha+\epsilon)-D-m_a\sin\gamma\left(g+\frac{\beta n}{m}V^2\right) \qquad (3.7)$$

The drag term, D, is also an function of α so the solution for alpha is given by the transcendental equation above.

In order to solve for an angle of attack to be used throughout the maneuver, an initial value must be selected and the above equation (3.7) must be iterated to solve for α at each successive time interval. As shown in Reference 3, Newton's Method of convergence was used to arrive at an angle of attack for this situation. Initially guessing α involved using a binomial curve fit for the drag versus angle of attack data. Assuming minimal values for the tangential acceleration and angle of attack (so that the cosine is nearly equal to

one) and no thrust vector angle in Equation 2.11, then the thrust is equal to the drag (or the binomial expansion curve fit for drag),

$$\frac{T}{\frac{1}{2}\rho V^2 S} = C_4 + C_5\alpha + C_6\alpha^2 \tag{3.8}$$

where C_4, C_5, and C_6 are the coefficients for the zeroth, first and second order terms, respectively, in the binomial curve fit expression [Ref. 3: p. 13]. The quadratic formula gives a method for calculating the first guess for α.

$$\alpha = \frac{C_5 + \sqrt{C_5^2 + 4\left[\frac{T}{\frac{1}{2}\rho V^2 S} - C_4\right]C_6}}{2C_6} \tag{3.9}$$

This technique is used in the computer program to simulate the aerobang maneuver to get a satisfactory approximation for the varying angle of attack.

D. THE HEATING RATE PROFILE

The previous thesis examined the aerocruise and aerobang at only two heating rate values. It was assumed that the resulting regions of superior performance for both subcircular and supercircular speeds held for all heating rates in between [Ref. 3: p. 63].

Prior to a closer examination of the behavior of flight parameters for the aerobang maneuver, this assumption was validated by determining the velocities at which aerocruise

lost its superiority to aerobang in terms of the inclination changes produced during the 2% mass fraction runs. These results, shown in Figure 6, do show that at very near circular speeds, the aerocruise maneuver did produce better results, but that the profile is not entirely symmetrical about the circular velocity. In general it was true that, at lower heating rates, the aerocruise method was better for a much smaller range of velocities.

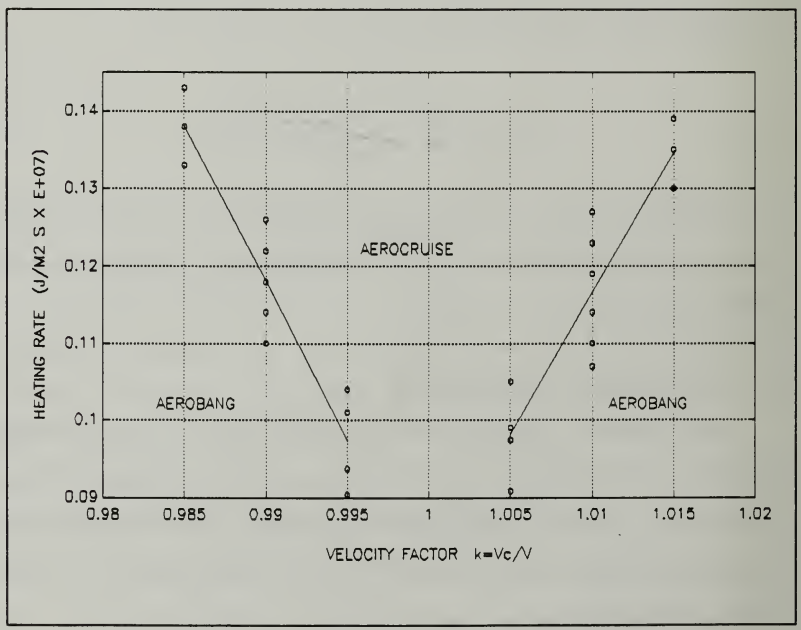

Figure 6 Aerobang and Aerocruise Efficiency Velocities and Heating Rates

IV. SIMULATION PROGRAM

In order to evaluate the potential of the aerobang orbital plane change maneuver, a FORTRAN program, previously developed [Ref. 3], was modified and used to simulate the action of the spacecraft while in the atmosphere. The modifications to the original program included the addition of ε, the thrust vector angle, the addition of a constant angle of attack option, and the elimination of the aerocruise option and the associated calculations.

The program, listed in Appendix A, was written in a modular format, using several subroutines for calculations, integration of the equations of motion, and output. The main program calls each one and controls their use in the program. For the heating rate versus velocity simulations used in Chapter III, the original program [Ref 3; App. A] was used to produce the aerocruise data shown in Figure 6.

A. THE MAIN PROGRAM

The main portion of the program links the subroutines together and controls the iteration of the solution. The two input files and one output file (also in Appendix A) are opened first. The use of the two input files (AERO.DAT and DATA.DAT) minimized the changes that had to be made to the program and subroutines themselves. The AERO.DAT file

contains the information about the spacecraft and the DATA.DAT file contains the information concerning the flight profile and the printing interval. The main program also calculates the mass changes throughout the simulation and stops the program when the final mass is reached or if the time extends beyond the maximum allowed. A flow chart for the main program appears in Figure 7 [Ref. 3].

B. THE SUBROUTINES

1. The CNTRL Subroutine

The control subroutine is the major subroutine, calculating the atmospheric and heating rate models, as well as the angle of attack for the aerobang control itself. The angle of attack is computed using the Newton approximation routine as discussed in Chapter II to simulate the modulation of the angle of attack for the aerobang maneuver. Alternatively, the angle of attack can be fixed and allowed to change the heating rate accordingly. In either case, the lift and drag forces are calculated here for use later in the equations of motion. Figure 8 shows the flow chart for this subroutine.

2. The ACEL Subroutine

This subroutine computes the three accelerations, defined by Equations 2.10, 2.11, and 2.12. These values are used in the next subroutine to evaluate the motion of the spacecraft.

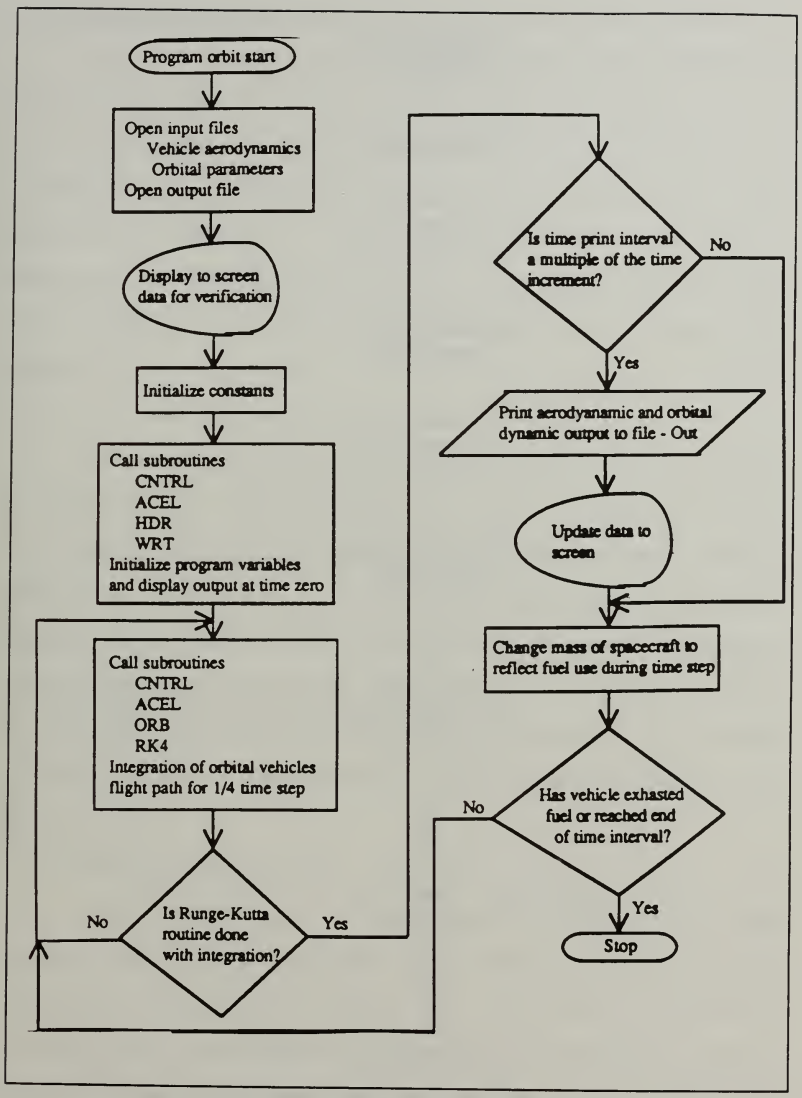

Figure 7 Flow Chart for the Main Program

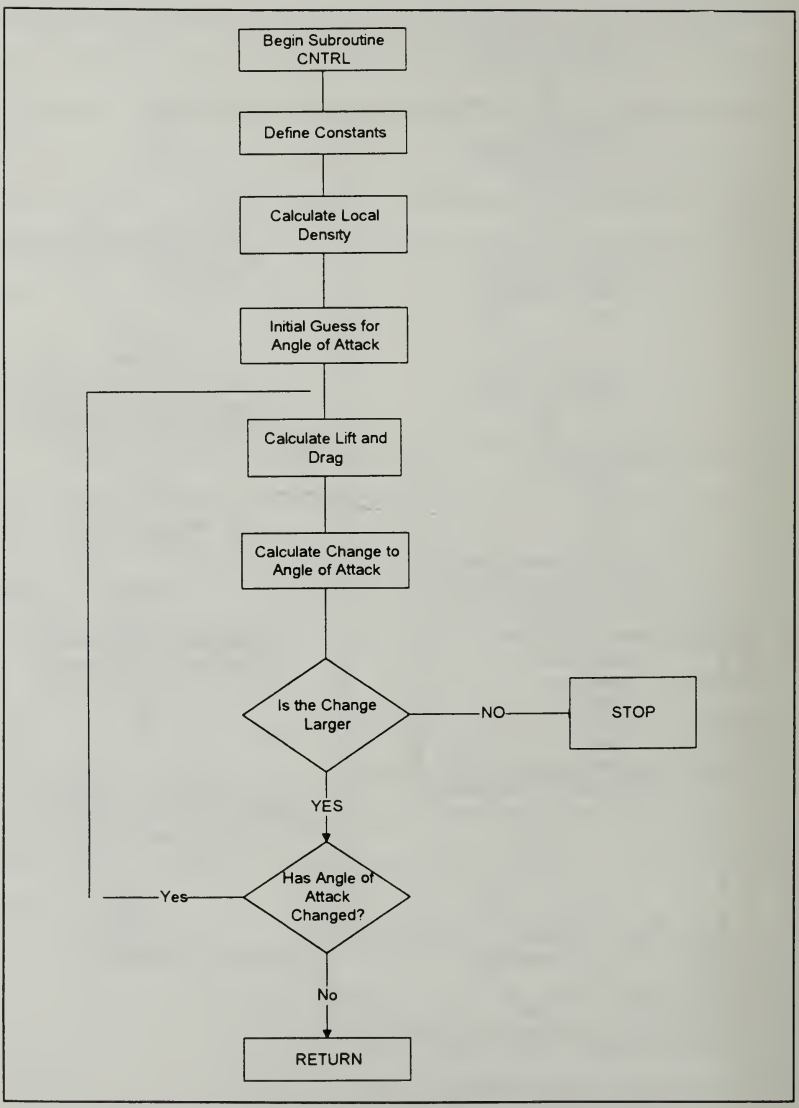

Figure 8 Flow Chart for Subroutine CNTRL

3. The ORB Subroutine

In this portion of the program, the six equations of motion (Equations 2.1, 2.2, 2.3, 2.13, 2.14, and 2.15) are defined in terms of the six variables defining the motion of the spacecraft; given as a vector, X(6), along with their derivatives, XDOT(6). These variables are used in the subroutine to compute the motion of the spacecraft at each time iteration. The equations are integrated in a Runge-Kutta routine, described later.

4. The WRT and HDR Subroutines

These subroutines control the output of the program. The HDR (header) routine creates a header in the output file that gives the initial conditions of the program and the headers for the columns of data that the program computes. The WRT (write) subroutine is called from the main program and used on each time iteration to write the calculated data into the output file. It is also called at the beginning and end of the iterations to put both the initial and final data rows into the file.

5. The RK4 Subroutine

This subroutine is the fourth order Runge Kutta routine used to integrate the equations of motion. It was written by Professor I. M. Ross and is a part of the public collection of subroutines at the Naval Postgraduate School. Here, the time iterations are counted and used to create the

multiple integration computations and send the results to the main program for writing into the output file.

C. PROGRAM VERIFICATION

Since this program is based on an earlier version, the validation of this program involved using it to verify results obtained in the previous study. By setting the thrust vector angle equal to zero in the AERO.DAT file's last entry, the exact same results should be obtained for similar initial conditions used previously.

The comparison of the aerobang and aerocruise maneuvers to verify the applicability of aerobang over the original heating rate profile provided an opportunity to verify the program's proper operation. By using both programs to calculate results for the aerobang cases and obtaining the same results, the new program could then be used on its own to incorporate the effects of thrust vector control and serve as a tool for further analysis of the aerobang maneuver.

V. AEROBANG PERFORMANCE ANALYSIS

As shown in Chapter III and previous studies [Ref. 3], there exist certain conditions in which the aerobang orbital plane change is the most efficient as determined by the amount of orbital inclination change that can be achieved for a given amount of fuel expended. Having determined the conditions necessary for successful aerobang maneuvers, the next step is to determine the ways in which the aerobang maneuver can be improved and best utilized to achieve a given mission criterion. The effects of adding a thrust vector control (TVC) system to improve upon previously obtained optimization results was examined first. Further simulations focused on the effects of increasing the mass fraction of fuel burned to allow for more useful inclination changes (on the order of ten or more degrees per maneuver) and the advantages and disadvantages of fixing the angle of attack rather than the heating rate for a specific maneuver.

In order to remain consistent with the previous study [Ref. 3] and to be able to compare the previous results with those obtained and given here, a review of those results is necessary.

The previous thesis looked at both subcircular and supercircular velocities for both aerocruise and aerobang maneuvers for two distinct heating rates. The effects of the

heating rate values over the entire range rather than just the two endpoints on the viability of both subcircular and supercircular results were discussed in Chapter III. These results were based on a mass fraction of fuel expended of only two percent.

For the higher heating rate (1.42×10^6 W/m^2), the best aerobang performance results, in terms of inclination changes, occurred at a velocity factor ($k=V_c/V$) of 0.98 for the supercircular case and 1.02 for the subcircular case, with inclination changes of 0.554° and 0.789°, respectively.

A. THRUST VECTOR CONTROL

1. Subcircular Case

In order to determine the overall effects of thrust vector control on the aerobang maneuver, the computer simulations were run for a range of ε from -80 to 80 degrees. While these angles may not presently be feasible from a structural or control point of view, they were included for completeness. The simulations were run at an initial radial distance of 6447 km, corresponding to an altitude of 77 km, and a heating rate of 1.42 MW/m^2. As shown in Figure 9 below, the most efficient value for ε fell between 10° and 16°, giving an inclination change of 0.8° over that range of vectoring angles. For negative values of thrust vector angles, the inclination changes were not as large as those at zero and positive angles since negative values of ε will have a

component in the direction directly opposing the lift which is responsible for the change in inclination.

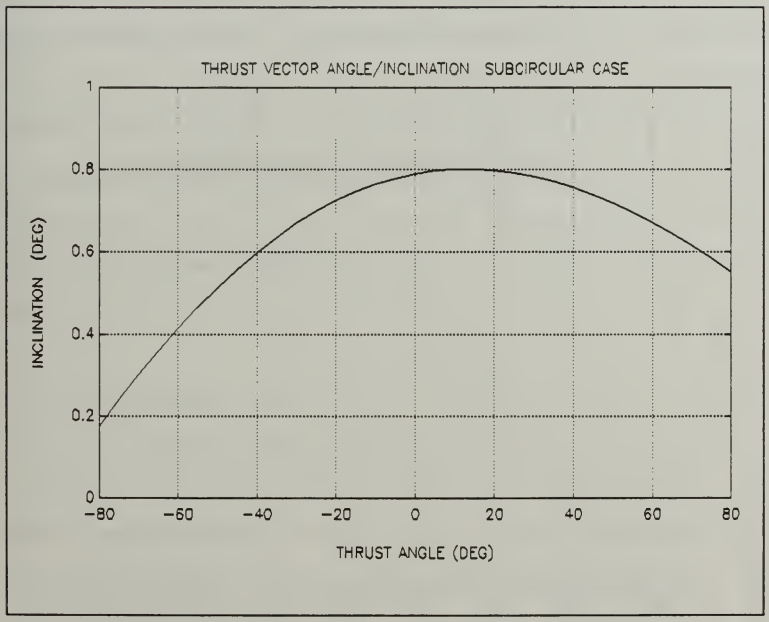

Figure 9 Thrust Vector Angle Effects - Subcircular Case

2. Supercircular Case

For k = 0.98, at the same altitude and heating rate, similar results were obtained for the addition of thrust vectoring for this case. As shown in Figure 10, the best inclination change occurred with a thrust vector angle of 15 to 20 degrees, resulting in an inclination change of 0.570°. At higher ε, the angles of attack decreased as the spacecraft moved faster to higher less dense air with a subsequent loss of lift.

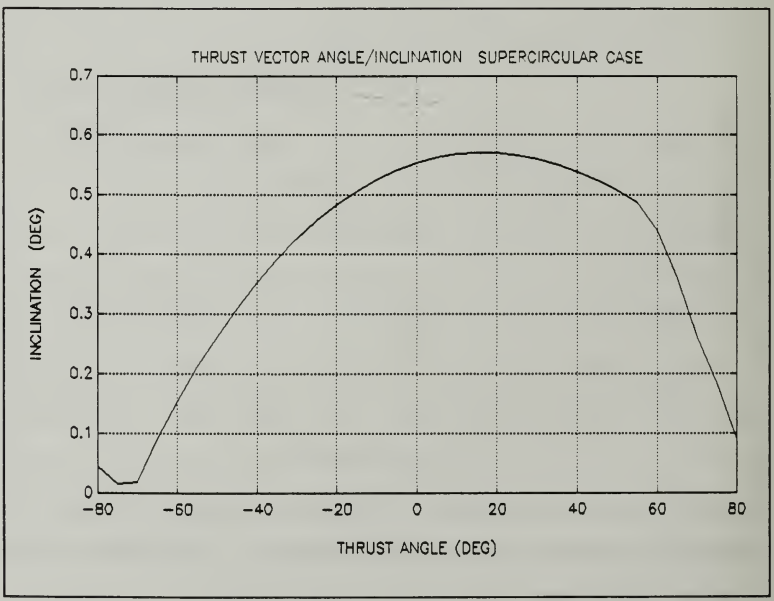

Figure 10 Thrust Vector Angle Effects - Supercircular Case

The shape of the curve over the broad range of thrust vector angles is again indicative of the effects of extreme values of ε on flight performance.

B. INCREASING FUEL MASS FRACTION

It would be logical to conclude that by increasing the amount of fuel consumed for an aerobang maneuver, a greater change in inclination would be achieved. By establishing a goal of achieving an inclination change of 10° or more, the effects of increasing the allowable mass fraction were investigated. These simulations were run for both subcircular and supercircular orbits (k=1.02 and 0.98), at an initial altitude of 77 km (R=6447 km), and restricted to the same heating rate as was used in the previous 2% fuel mass fraction runs.

1. Subcircular Case

a. Constant Heating Rate

Initially, the increase of mass fraction was tried for the constant heating rate case usually prescribed for the aerobang maneuver. As the mass fraction was increased from the original 2% up to 20%, it became apparent that the technique of modulating the angle of attack to maintain a constant heating rate profile was difficult to implement.

Figure 11 shows the expected effect of increasing mass fraction on aerobang maneuvers. The inclination change is

very impressive, between 25° and 28°, depending upon the thrust vector angle. In these simulations, five values of ε (0, 10, 20, 30, and 40°) were used to show the effects of TVC on these extended runs. The thrust vector angle labels for this figure refer to the right hand side of the curves; zero at the top, 40 at the bottom. The smaller values of ε, gave the greater inclination changes. While this seems to contradict the 2% mass fraction results, the data for time values less than 60 seconds revealed that the behavior of the inclination followed the behavior shown earlier for the 19 second, 2% mass fraction case. The $\varepsilon = 10°$ curve starts out above the 0° curve, but the curves cross at 56 seconds and the 0° curve finishes slightly above the 10° curve. The two curves are nearly indistinguishable from each other, but the results for the 2% case (the slight advantage of the ten degree thrust angle with the three other cases even lower) are shown in Figure 12 and are consistent with the results for the longer times of Figure 11.

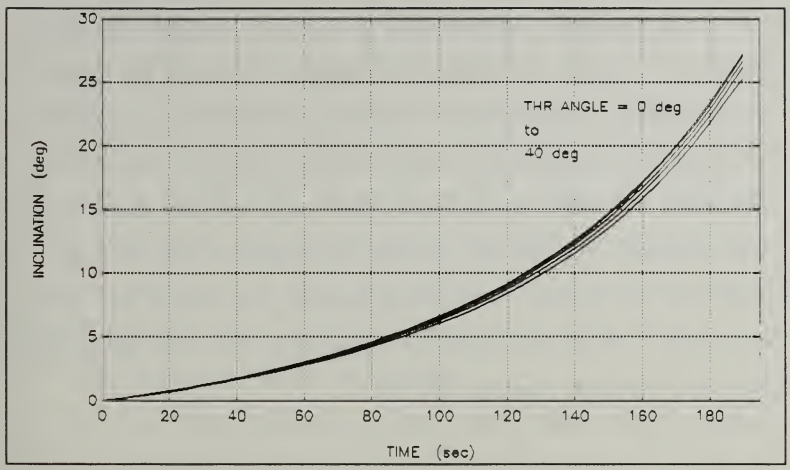

Figure 11 Inclination For Constant Heating Rate

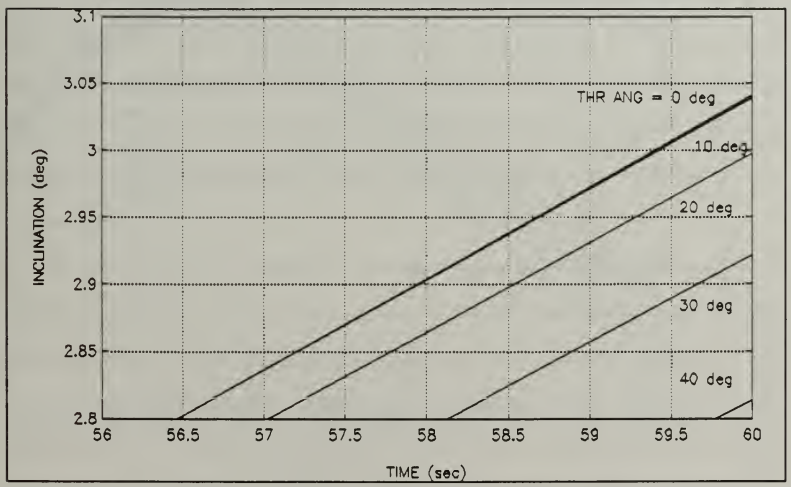

Figure 12 Magnification of the Constant Heating Rate Inclination

This superior performance in orbit transfer comes with a penalty. Figure 13 shows the change in angle of attack over the extended simulations. Values of α rise to between 65 and 70 degrees, depending again on the thrust vectoring, and decrease to about 53 or 54°. The zero thrust angle case had the highest angles of attack throughout the flight. The addition of thrust vectoring caused the angle of attack to decrease. This reduction in α reduced the lift generated and the inclination changes as well.

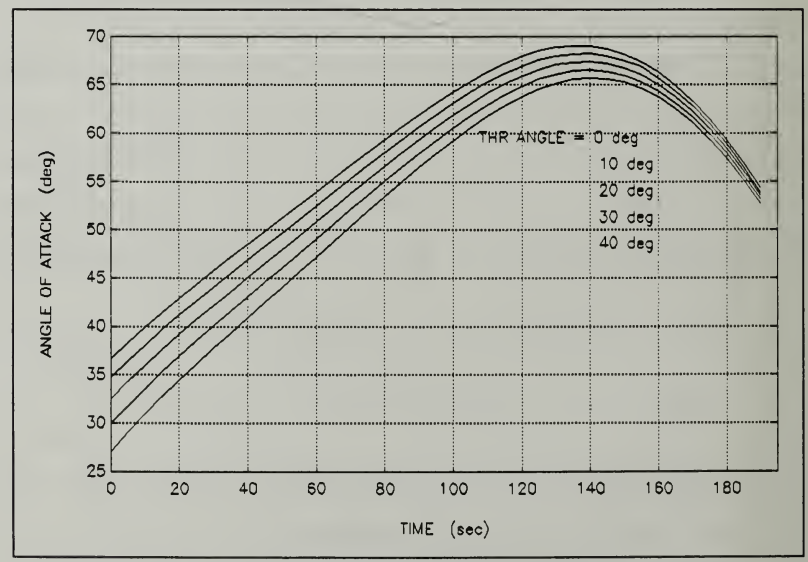

Figure 13 Angles of Attack For Constant Heating Rate

The aerodynamic data provided for the MRRV, mentioned in Chapter I, only covered angles of attack of up to 40°. It can be assumed, therefore, that the vehicle is probably not capable of flying at α's greater than 40°. If that is the case, then a vehicle of the same surface area, initial mass, fuel burning rate, and thrust would not meet these high angle of attack results, if they are valid, while maintaining the constant heating rate profile simulated in this study.

b. Constant Angle Of Attack

At this point, a departure from the standard aerobang maneuver theory was attempted to try to avoid the angle of attack problems described above. Rather than allowing the angle of attack to vary and allowing the constant heating rate control the maneuver, the angle of attack was fixed and the heating rate was allowed to vary to evaluate the possible inclination changes while observing the heating rate to see if it would exceed the desired heating rate and, if so, by how much.

An inclination change of approximately 10° was still a goal and several values of α were tested to see if this goal could be met. The graphs in Figures 14, 15, and 16 show the results of these runs. Angles of attack of 30°, 35°, and 40°, respectively, were selected to get the desired ten degree inclination change. Again, the same five values of thrust vectoring are included to show their effects. As α increases,

the inclination changes rise from values of 6.5° to 9.5° at α = 30° to values of 12° to 17° at α = 40°. In this case, the increasing thrust angle with the fixed angle of attack resulted in increasing inclination changes throughout the runs. With α fixed, its contribution to the vehicle's lift is fixed and the changes in inclination for this case are made by the contribution of the thrust vectoring to the lift generated.

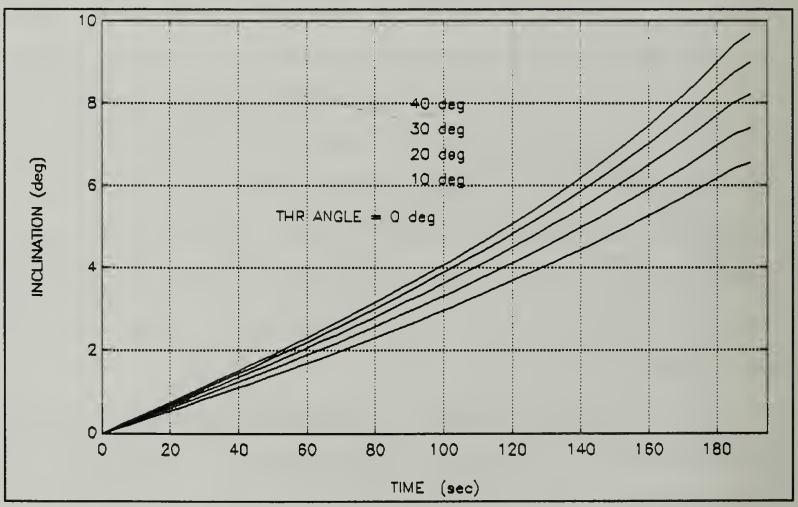

Figure 14 Inclination For 30° Angle of Attack

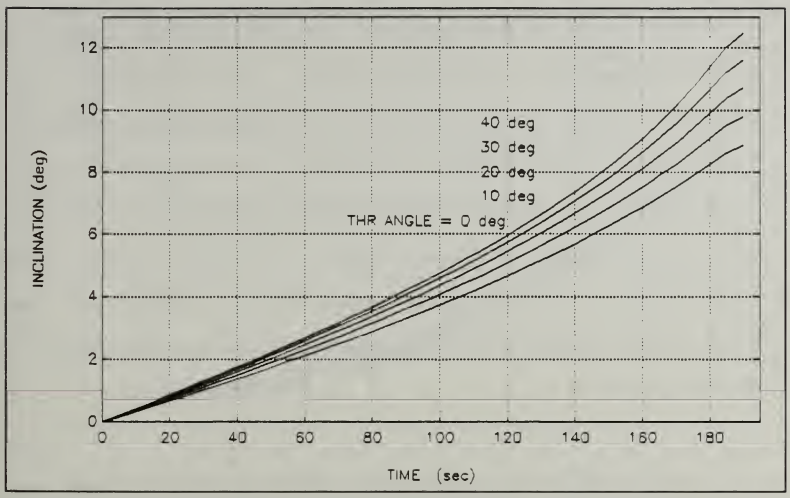

Figure 15 Inclination For 35° Angle of Attack

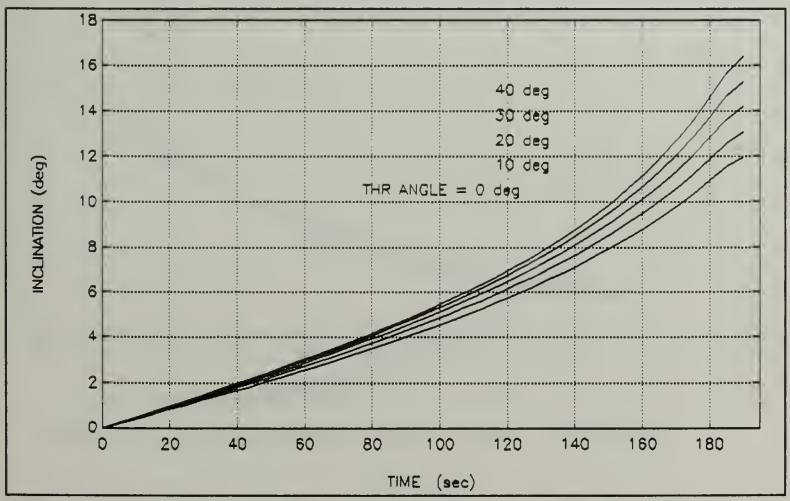

Figure 16 Inclination For 40° Angle of Attack

The result of more concern is that of the heating rates that existed as a result of the fixed α flight regime. Figures 17, 18, and 19 show the heating rates obtained for these simulations. They vary from 1.8×10^6 W/m^2 on up to 2.2×10^6 W/m^2, both significantly above, almost up to twice the value used for all previous runs. A vehicle used to perform these fixed α aerobang maneuvers would, therefore, need to have a thermal protection system capable of withstanding these heating rates.

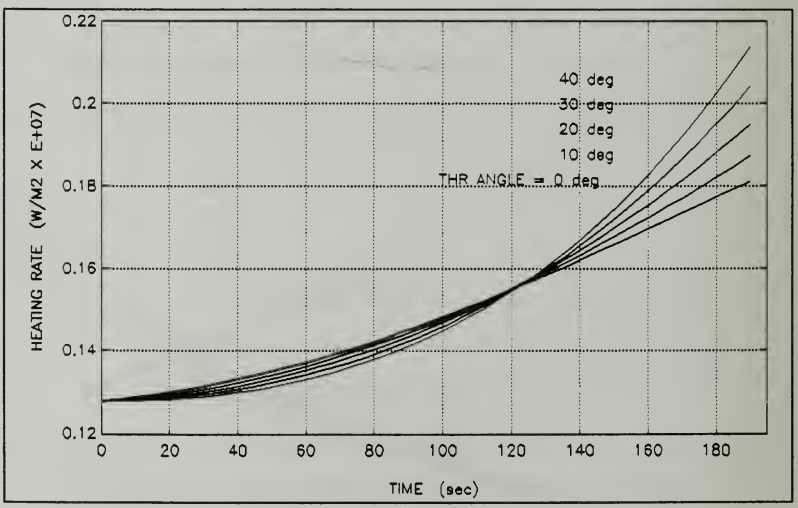

Figure 17 Heating Rate For 30° Angle of Attack

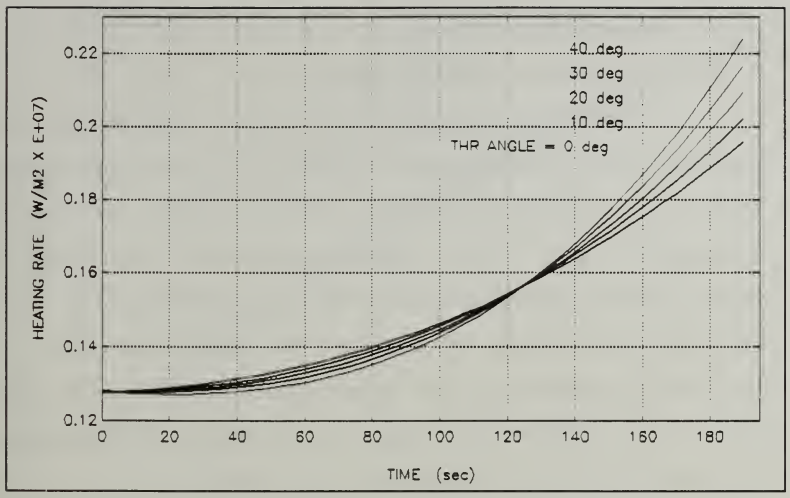

Figure 18 Heating Rate For 35° Angle of Attack

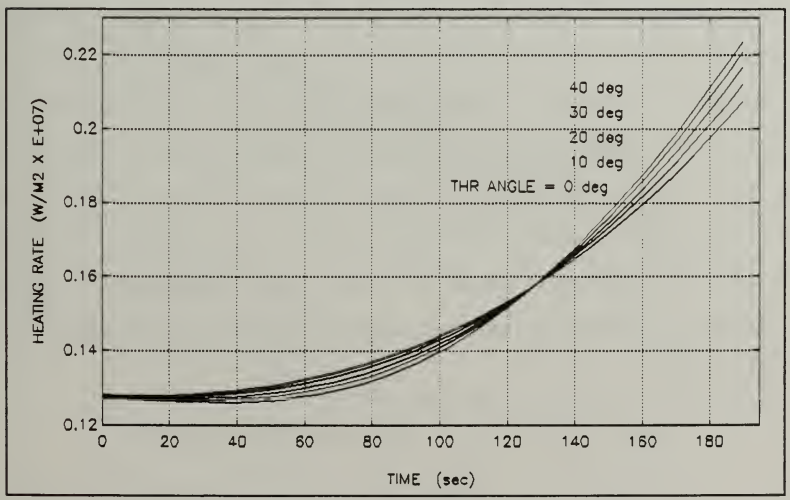

Figure 19 Heating Rate For 40° Angle of Attack

2. Supercircular Case

a. Constant Heating Rate

Supercircular aerobang maneuver simulations using 20% fuel mass fraction were attempted over the same range of angles of attack and thrust vector angles as for the subcircular case. Under otherwise identical conditions, the supercircular simulations were unable to generate any results that were even close to those of the subcircular case. The inclination changes were no greater than 0.865° for an ε of 10° and the burn time was no more than 37 seconds, approximately 4% mass fraction as opposed to the desired 20% set in the simulation program. The combination of decreasing α and increasing altitude at the supercircular velocity caused the vehicle to lose its lifting force, resulting in the shortened flight. Compared to the subcircular case, the supercircular aerobang maneuvers proved to be ineffective in producing substantial inclination changes (on the order of 10°) for any kind of significant increases in fuel mass fraction, although they may still be viable for short, quick maneuvers. Figures 20 and 21 show the inclination and angle of attack results for this case.

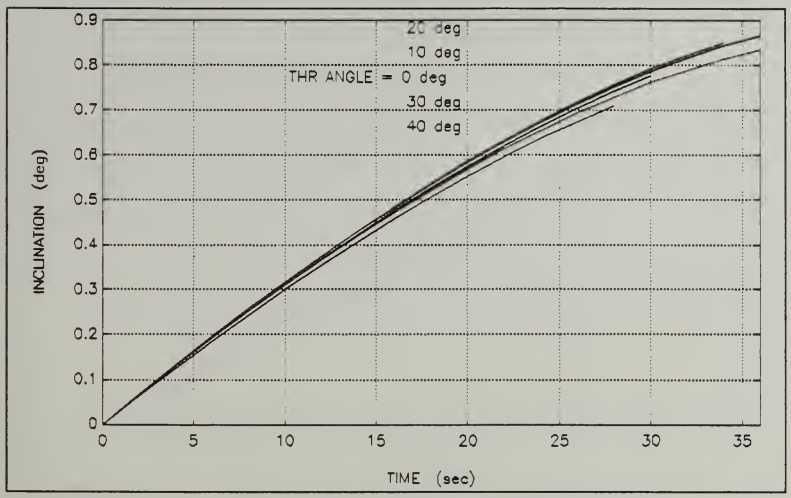

Figure 20 Inclination for Constant Heating Rate

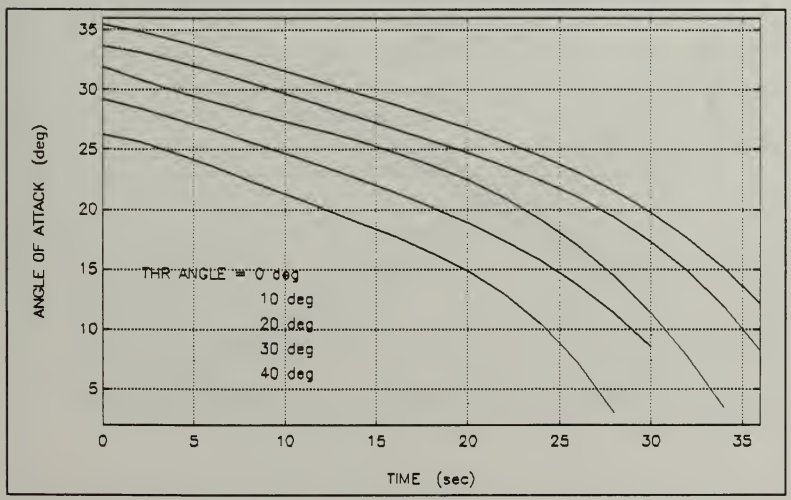

Figure 21 Angles of Attack For Constant Heating Rate

b. Constant Angle of Attack

This case proved to be more successful since the angle of attack (and therefore the lift generated) never decreased to the values near zero as it did in the constant heating rate case. Each aerobang simulation was completed for the entire 20% burn and significant inclination changes were observed. Figures 22, 23, and 24 show these results.

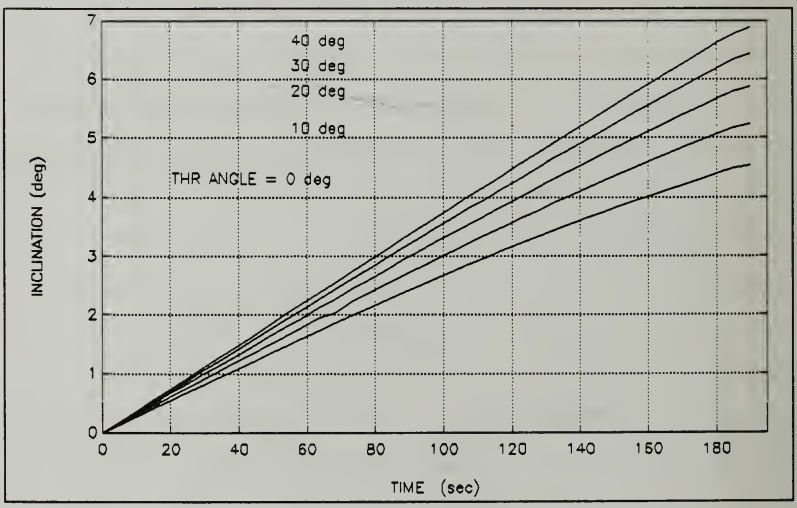

Figure 22 Inclination for 30° Angle of Attack

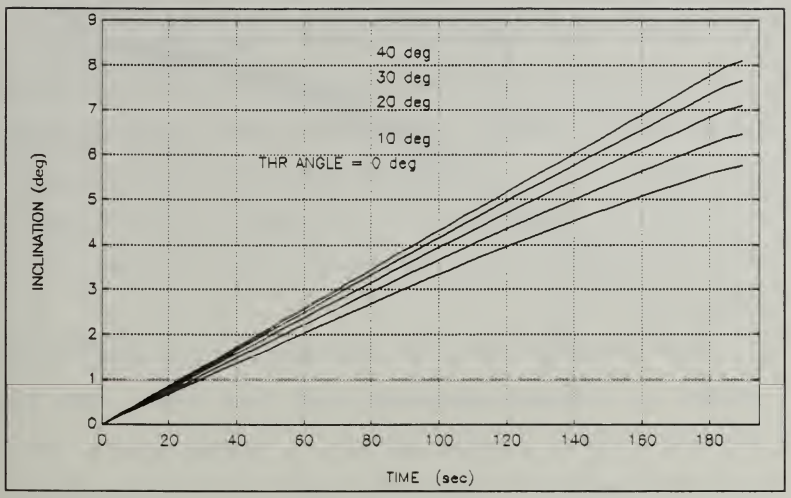

Figure 23 Inclination For 35° Angle of Attack

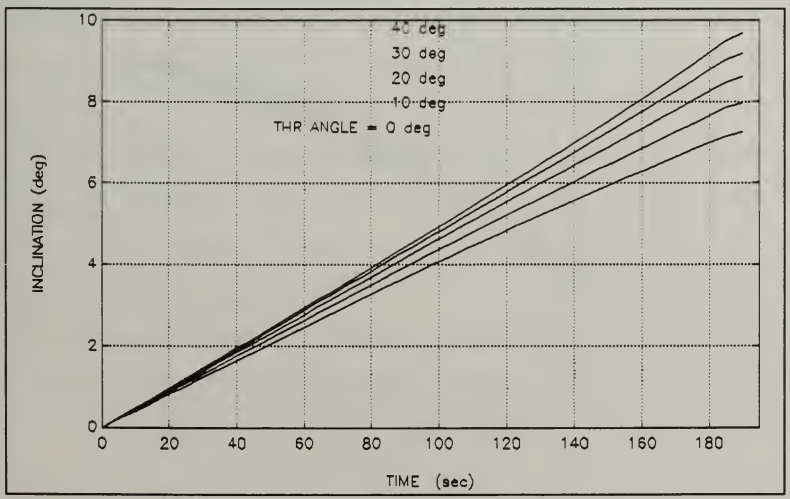

Figure 24 Inclination For 40° Angle of Attack

As in the subcircular case, the inclinations here increased with higher angle of attack and with increased thrust vector angles. The maximum values, however, were not as large since the supercircular trajectories caused the altitude of the vehicle to increase and the resulting atmospheric density to decrease, thus reducing the lift capability.

The heating rates for supercircular flights, however, showed an inherent advantage with this case. The higher altitudes had a greater effect on heating rates than the increased velocities did, resulting in decreasing values for heating rate. As shown in Figures 25, 26, and 27; the heating rates for all cases started with the same value of 1.45×10^6 W/m^2. The final values depend on both angle of attack and thrust vector angle. The higher angle of attack cases resulted in less pronounced decreases in heating rate value from start to finish. The thrust vector angles in these cases actually contributed to higher heating rates as well, due to the slight increase in lift and velocity that they provided. In particular, as seen in Figure 27, a limit is reached in the 40° thrust vector case, where the heating rate reaches a minimum limit and then begins to increase again.

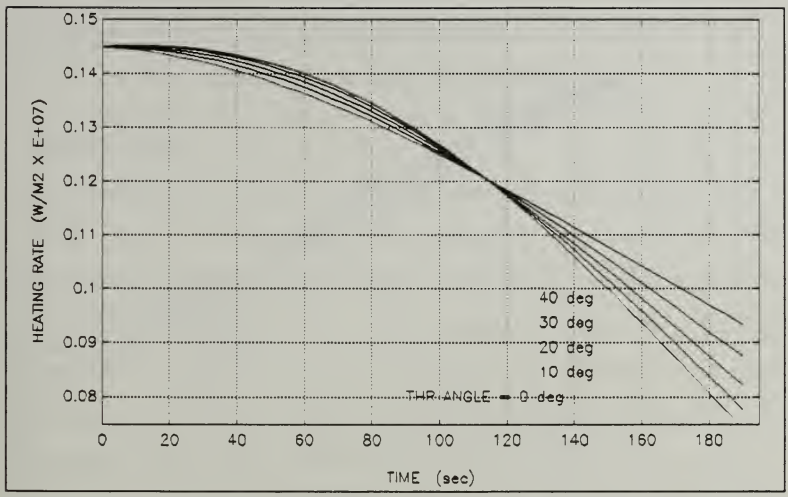

Figure 25 Heating Rates For 30° Angle of Attack

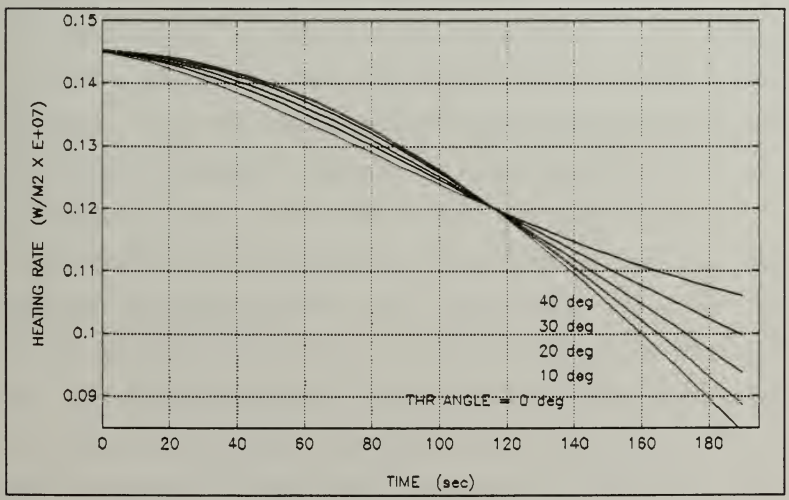

Figure 26 Heating Rates For 35° Angle of Attack

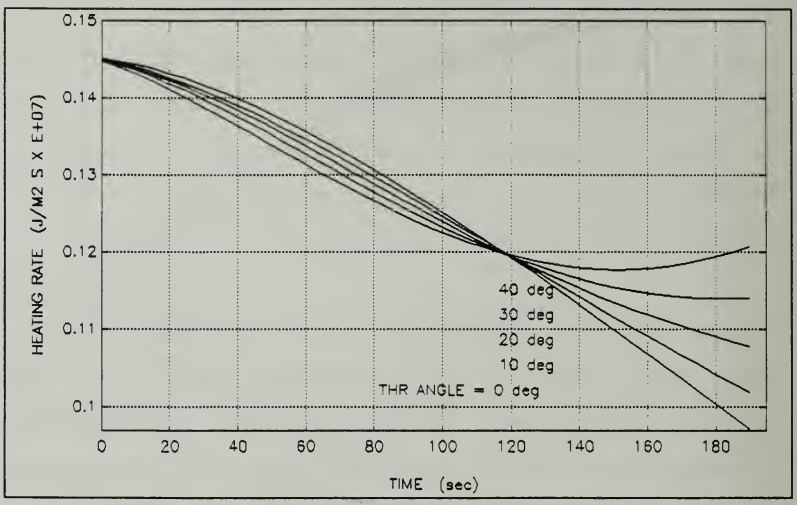

Figure 27 Heating Rates For 40° Angle of Attack

VI. CONCLUSIONS AND RECOMMENDATIONS

A. CONCLUSIONS

The aerobang orbital plane change maneuver has been shown to have both commercial and military applications for obtaining significant inclination changes for aerodynamically assisted orbital transfers. The improved efficiency of the aerobang technique over the aerocruise for subcircular and supercircular speeds at two discrete heating rate values given in Reference 3 was shown here to extend to the entire range of heating rates studied, not just the high and low heating rate cases.

Thrust vector control can be effective in increasing inclination changes for both short and long duration aerobang maneuvers. This was demonstrated for both supercircular and subcircular velocities. The use of thrust vector control was most effective when applied at a constant angle of attack.

The effects of increasing mass fraction of fuel consumed from two to twenty percent had a significant effect on the aerobang maneuver, beyond the obvious extension of the time used to perform the maneuver. For the subcircular maneuvers, the constant heating rate method of controlling the aerobang flight resulted in excellent inclination changes but with extremely high (70°) angles of attack. By controlling the

angles of attack, the heating rates increase by nearly a factor of two, placing new requirements on any spacecraft design.

The supercircular aerobang maneuvers were also simulated for both constant heating rate and constant angle of attack cases. The constant heating rate case proved to be ineffective in generating even one degree of inclination change because of the loss of angle of attack and, therefore, lift. The constant angle of attack runs, however, proved to be almost as effective as for the subcircular cases. This case also provided two inherent advantages over the subcircular case, an increasing altitude which translates to a decreasing heating rate value and the likelihood of an easier reorbit maneuver.

B. RECOMMENDATIONS

There remain several areas in the study of aerodynamically assisted orbital plane change maneuvers that have yet to be explored. Among these are the effects of combining any two or all of the three techniques (aeroglide, aerocruise, and aerobang) to maximize the fuel efficiency of a given inclination change requirement.

This thesis, as well as most other work in this area, deals only with the atmospheric passage portion of the orbit transfer. By extending the simulations to cover an entire orbit transfer, including both entering and exiting the

atmosphere, a better measure of the effectiveness of these maneuvers can be made.

This is the first work in which the constant angle of attack method of controlling the aerobang maneuver was used. Further studies should concentrate on whether or not it can indeed be a viable means of control, from both a flight control system and thermal protection point of view.

In order to verify the applicability of aerodynamically assisted maneuvers, the study of thermal protection system requirements and techniques must be included. Superior atmospheric and heating models can also be used to refine the requirements for such systems.

Finally, a means of minimizing the time required for a maneuver to meet a given inclination change requirement could be established. This would allow the mission goal to be met while minimizing the integrated heat load on the spacecraft.

APPENDIX A

```
      PROGRAM ORBIT
      IMPLICIT REAL*8(A-H,L-Z)
      DIMENSION X(6),XDOT(6),C(6)
C
C     PROGRAMMER: THOMAS P. SPRIESTERBACH
C     MODIFIED BY:  RICHARD E. JOHNSON
C     DATE      : 15 FEB 93
C     SYSTEM    : IRIS INDIGO/FORTRAN
C
C
C                              VARIABLE LIST
C
C     I           COUNTING INDEX
C     INDEX       COUNTING INDEX FOR RUNGE-KUTTA ROUTINE
C     J           COUNTING INDEX
C     KOUNT       COUNTING INDEX FOR OUTPUT DETERMINATION
C     DUM         DUMMY VARIABLE FOR CONVENIENCE
C     OLDCO       CONTROL VARIABLE FOR CONVERGENCE ON ANGLE OF
C                 ATTACK [AOA]
C     CHANGE      INCREMENTAL CHANGE IN AOA USING NEWTONS METHOD
C     NE          NUMBER OF EQUATIONS OF MOTION
C     T           TIME                                        (SEC)
C     TF          FINAL TIME                                  (SEC)
C     H           INCREMENT OF TIME [RUNGE-KUTTA ROUTINE]     (SEC)
C     TPI         TIME PRINT INTERVAL                         (SEC)
C     X(1)        RADIUS                                      (METERS)
C     X(2)        THETA                                       (RADIANS)
C     X(3)        PHI                                         (RADIANS)
C     X(4)        VELOCITY                                    (M/SEC)
C     X(5)        FLIGHT PATH ANGLE GAMMA                     (RADIANS)
C     X(6)        PSI                                         (RADIANS)
C     XDOT()      DERIVATIVES OF THE ABOVE SIX VARIABLES
C     C(1)        ZEROTH ORDER COEFFICIENT FOR CL EQUATION
C     C(2)        FIRST ORDER COEFFICIENT FOR CL EQUATION
C     C(3)        SECOND ORDER COEFFICIENT FOR CL EQUATION
C     C(4)        ZEROTH ORDER COEFFICIENT FOR CD EQUATION
C     C(5)        FIRST ORDER COEFFICIENT FOR CD EQUATION
C     C(6)        SECOND ORDER COEFFICIENT FOR CD EQUATION
C     BETA        DENSITY MODEL EXPONENT                      (METERS)
C     G0          GRAVITY AT EARTH SURFACE                (9.806M^2/S)
C     G           LOCAL GRAVIATIONAL ATTRACTION               (M^2/S)
C     H0          REFERENCE ALTITUDE FOR DENSITY MODEL        (METERS)
C     RHO0        REFERENCE DENSITY FOR DENSITY MODEL         (KG/M^3)
C     MU          GRAVITATIONAL CONSTANT
```

```
C     ALPHA      ANGLE OF ATTACK                              (RADIANS)
C     ALFA       ANGLE OF ATTACK                               (DEG)
C     VEC        THRUST VECTORING ANGLE                        (DEG)
C     EPS        THRUST VECTORING ANGLE                       (RADIANS)
C     MASS       MASS OF SPACECRAFT                            (KG)
C     MASS0      INITIAL MASS OF SPACECRAFT                    (KG)
C     SPI        SPECIFIC IMPULSE OF POWER PLANT               (SEC)
C     R          RADIUS                                        (M)
C     V          VELOCITY                                      (M/S)
C     RADIUS     RADIUS                                        (KM)
C     VELOCITY   VELOCITY                                      (KM/S)
C     GAMMA      FLIGHT PATH ANGLE                             (DEG)
C     ANGM       ANGULAR MOMENTUM                              (M^2/S)
C     SIGMA      ANGLE OF BANK                                 (DEG)
C     OINC       INCLINATION                                   (DEG)
C     DELTA      INTERMEDIATE ANGLE                            (DEG)
C     OMEGA      LONGITUDE OF THE ASCENDING NODE               (DEG)
C     AS         TANGENTIAL ACCELERATION                       (M/S^2)
C     AR         RADIAL ACCELERATION                           (M/S^2)
C     AW         BINORMAL ACCELERATION                         (M/S^2)
C     THR        THRUST                                        (N)
C     AOB        ANGLE OF BANK                                (RADIANS)
C     RHO        DENSITY                                       (KG/M^3)
C     S          REFERENCE AREA OF SPACECRAFT                  (M^2)
C     N          DENSITY COEFFICIENT FOR HEATING RATE EQUATION
C     M          VELOCITY COEFFICIENT FOR HEATING RATE EQUATION
C     HEAT       STAGNATION POINT HEATING RATE          (WATTS/M^2)
C     QS         DYNAMIC PRESSURE TIMES THE REFERENCE AREA (N*M^2)
C     CD         COEFFICIENT OF DRAG
C     CL         COEFFICIENT OF LIGT
C     LIFT       LIFT ON SPACECRAFT                            (N)
C     DRAG       DRAG ON SPACECRAFT                            (N)
C
CCCCCCCCCCCCCCCCCCCCCCCCCCCCCCCCCCCCCCCCCCCCCCCCCCCCCCCCCCCCCCCCCCCCCCC
C
C      DEFINED FUNCTION FOR ACCEL DUE TO GRAVITY
C
      G(R)=MU/(R*R)
C
CCCCCCCCCCCCCCCCCCCCCCCCCCCCCCCCCCCCCCCCCCCCCCCCCCCCCCCCCCCCCCCCCCCCCCC
C
C
C      OPEN TWO INPUT FILES.....DATA.DAT    -  ORBITAL PARMS
C                               AERO.DAT    -  VEHICLE PARMS
C           ONE OUTPUT FILE......OUT.DAT    -  TABLE OF VALUES
C
CCCCCCCCCCCCCCCCCCCCCCCCCCCCCCCCCCCCCCCCCCCCCCCCCCCCCCCCCCCCCCCCCCCCCCC
C
C
      OPEN(10,FILE='data.dat', STATUS='OLD')
      OPEN(12,FILE='aero.dat',STATUS='OLD')
```

```
      OPEN(13,FILE='out.dat', STATUS='NEW')

      READ(10,1)(X(I),I=1,6),T,TF,H,TPI
1     FORMAT(/,/,20X,10(/,20X,D13.7))

      READ(12,2)(C(I),I=1,6),AOPT,AOB,N,M,S,MASS0,FM,SPI,THR,EPS
2     FORMAT(/,/,/,/,16(/,20X,D13.7))

C
C      NUMBER OF EQUATIONS TO INTERGRATE
C      X(1)....RADIUS
C      X(2)....THETA (SPHERICAL COORD. PARAMETER)
C      X(3)....PHI   (SPHERICAL COORD. PARAMETER)
C      X(4)....VELOCITY
C      X(5)....FLIGHT PATH ANGLE GAMMA
C      X(6)....PSI
C
C      INITIALIZATION OF CONSTANTS
C
      NE=6
      PI=3.14159265359D+0
      MU=3.986012D+14
      G0=9.806D+0
      MASS=MASS0
      VEC=EPS*180./PI
C
C      MAIN PROGRAM
C
      INDEX=0
      KOUNT=1
C
C      INITIAL CALL TO GET ACCELERATIONS AND CONTROL VARIABLES
C      FOR FIRST OUTPUT
C
      CALL CNTRL(DRAG,LIFT,THR,ALPHA,AOB,X,MASS,S,C,N,M,RHO,EPS)
      CALL ACEL(AS,AR,AW,DRAG,LIFT,THR,EPS,ALPHA,AOB,MASS)

      CALL HDR(X(1),X(4),MASS,THR,VEC,X(5))
      CALL WRT(X,T,THR,MASS,ALPHA,AOB,RHO,N,M)

CCCCCCCCCCCCCCCCCCCCCCCCCCCCCCCCCCCCCCCCCCCCCCCCCCCCCCCCCCCCCCCCCCCCCCCCCCC
C
C
C      THIS IS THE MAIN BLOCK OF THE PROGRAM CALLING FIRST THE
C     CONTROL SUBROUTINE TO DETERMINE THE OUTPUT VARIABLES.  NEXT,
C      THE ACCELERATION ROUTINE CALCULATES THE RELATIVE
C     ACCELERATION TO THE VEHICLE, THEN THE DIFFERENTIAL EQUATIONS
C     OF MOTION ARE DEFINED AND A FOURTH ORDER RUNGE-KUTTA ROUTINE
C      IS USED TO INTEGRATE THEM. THIS BLOCK IS COMPUTED AT EACH
C      TIME INCREMENT H.
C
```

```
CCCCCCCCCCCCCCCCCCCCCCCCCCCCCCCCCCCCCCCCCCCCCCCCCCCCCCCCCCCCCCCCCCCCCCCCCCC

100   CALL CNTRL(DRAG,LIFT,THR,ALPHA,AOB,X,MASS,S,C,N,M,RHO,EPS)
      CALL ACEL(AS,AR,AW,DRAG,LIFT,THR,EPS,ALPHA,AOB,MASS)
      CALL ORB(X,XDOT,AS,AR,AW,G(X(1)))
      CALL RK4(T,X,XDOT,NE,H,INDEX)
      IF(INDEX .NE. 0) GO TO 100

C      DETERMINE IF TIME TO PRINT TO OUTPUT USING TIME PRINT
C      INTERVAL

200   IF(KOUNT .LT. IDNINT(TPI/H)) GO TO 300

      CALL WRT(X,T,THR,MASS,ALPHA,AOB,RHO,N,M)

C      PRINT STATUS TO TERMINAL

      WRITE(6,7)T,ALPHA,AOB
7     FORMAT('+',F8.1,1X,F6.3,1X,F6.3)

      KOUNT=0
300   KOUNT=KOUNT+1
C
C      CHANGE MASS OF S/C
C
      MASS=MASS-THR*H/(SPI*G0)
C
C      TWO TESTS EITHER CAN STOP THE PROGRAM. TEST FOR MASS LESS
C      THAN FINAL MASS AND ALSO IF TIME IS GREATER THAN FINAL TIME
C
      IF(MASS .GT. FM .AND. T .LE. TF) GO TO 100
C
C      PRINT OUTPUT AGAIN IF MASS SWITCH ENDED PROGRAM
C
      IF(MASS .LE. FM) CALL WRT(X,T,THR,MASS,ALPHA,AOB,RHO,N,M)
C
      END
CCCCCCCCCCCCCCCCCCCCCCCCCCCCCCCCCCCCCCCCCCCCCCCCCCCCCCCCCCCCCCCCCCCCCCCCCCC
C
C     THIS SUBROUTINE CALCULATES THE CONTROL OF THE FREE VARIABLES
C      DURING THE ATMOSHPHERIC FLIGHT.
C
CCCCCCCCCCCCCCCCCCCCCCCCCCCCCCCCCCCCCCCCCCCCCCCCCCCCCCCCCCCCCCCCCCCCCCCCCCC
C
      SUBROUTINE CNTRL(DRAG,LIFT,THR,ALPHA,AOB,X,MASS,S,
     *C,N,M,RHO,EPS)
      IMPLICIT REAL*8(A-H,L-Z)
      DIMENSION X(6),C(6)
C
      MU=3.986012D+14
      GAMMA=X(5)
```

```
      R=X(1)
      V=X(4)
C
C      COEFFICIENTS FOR AN EXPONENTIAL DENSITY MODEL
C      REFERENCE J MEASE 1976 US STANDARD ATMOSPHERE
C      RANGE 50KM TO 120KM
C
      BETA=1.41D-4
      RHO0=3.0968D-4
      R0=6.435D+6

      G=MU/(R*R)
      RHO=RHO0*EXP(-BETA*(R-R0))
      QS=.5D+0*RHO*V*V*S

C
C      FOR AEROBANG THE AOB IS SET AND THE ANGLE OF ATTACK IS
C      CONTROLLED TO FLY AT A CONSTANT HEATING RATE; THE ALTITUDE
C      AND VELOCITY ARE ALLOWED TO FLOAT.
C
C
C      GUESS ALPHA INITIALLY FOR NEWTON APPROXIMATION ROUTINE
C
      ALPHA=(C(5)*QS+SQRT(C(5)**2+4.*QS*C(6)*(THR*COS(EPS)
     * -QS*C(4))))/(2.*C(6)*QS)
C
C      USE NEWTON APPROXIMATION METHOD TO CONVERGE ON ALPHA.
C      USE A WHILE STRUCTURE FOR THE CONVERGENCE OF ALPHA.
C      SET OLDCO AND CHANGE EQUAL TO THE VALUES BELOW TO ENSURE
C      THAT THE PROGRAM SWITCHES ARE NOT INITIALLY TRIPPED.
C
      OLDCO=1.D+10
      CHANGE=1.
C
C     OR, ALLOW ALPHA TO BE A CONSTANT AND OBSERVE THE BEHAVIOR OF
C      THE HEATING RATE AND INCLINATION.
C
CC    ALPHA = 0.69813
C
      DO WHILE (ABS(CHANGE) .GT. 1.D-3)
      CL=C(1)+C(2)*ALPHA+C(3)*ALPHA**2
      CD=C(4)+C(5)*ALPHA+C(6)*ALPHA**2
C
C       CALCULATE THE LIFT AND DRAG FORCES FROM THE COEFFICIENTS
C       CALCULATED ABOVE.
C
      LIFT=CL*QS
      DRAG=CD*QS
C
C      THESE THREE EQUATIONS REPRESENT THE FUNCTION AND ITS
C      DERIVATIVE WITH RESPECT TO ALPHA FOR NEWTON'S METHOD OF
```

```
C      APPROXIMATION
C
       COEFF=(THR*COS(ALPHA+EPS)-DRAG)-MASS*SIN(GAMMA)
      **(G+BETA*(N/M)*V*V)
       COEFP=-THR*SIN(ALPHA+EPS)-(C(5)+2*C(6)*ABS(ALPHA))*QS
C
       CHANGE=COEFF/COEFP

       ALPHA=ALPHA-CHANGE
       IF (ABS(OLDCO)-ABS(CHANGE).LE.0.) STOP
       OLDCO=CHANGE
       END DO
       RETURN
       END
C
C
CCCCCCCCCCCCCCCCCCCCCCCCCCCCCCCCCCCCCCCCCCCCCCCCCCCCCCCCCCCCCCCCCCCCCCCCCC
C
C      THIS SUBROUTINE DEFINES THE TANGENTIAL, NORMAL, AND BINORMAL
C       ACCELERATIONS WITH RESPECT TO THE VEHICLE AND THE ORBITAL
C       PLANE.
C
CCCCCCCCCCCCCCCCCCCCCCCCCCCCCCCCCCCCCCCCCCCCCCCCCCCCCCCCCCCCCCCCCCCCCCCCCC
C
       SUBROUTINE ACEL(AS,AR,AW,DRAG,LIFT,THR,EPS,ALPHA,AOB,MASS)
       IMPLICIT REAL*8(A-H,L-Z)
C
C       COMPUTE THE ACCELERATIONS ON THE FLIGHT VEHICLE USING
C       THE THREE ACCELERATION EQUATIONS, WHICH INCLUDE THE
C       THRUST VECTORING ANGLES.
C
       AS=(THR*COS(ALPHA+EPS)-DRAG)/MASS
       AW=(LIFT+THR*SIN(ALPHA+EPS))*SIN(AOB)/MASS
       AR=(LIFT+THR*SIN(ALPHA+EPS))*COS(AOB)/MASS
C
       RETURN
       END
C
CCCCCCCCCCCCCCCCCCCCCCCCCCCCCCCCCCCCCCCCCCCCCCCCCCCCCCCCCCCCCCCCCCCCCCCCCC
C
C
C      THIS SUBROUTINE IS THE COLLECTION OF DIFFERENTIAL EQUATIONS
C       WHICH DESCRIBE THE MOTION OF THE SPACECRAFT.
C
CCCCCCCCCCCCCCCCCCCCCCCCCCCCCCCCCCCCCCCCCCCCCCCCCCCCCCCCCCCCCCCCCCCCCCCCCC
C
       SUBROUTINE ORB(X,XDOT,AS,AR,AW,G)
       IMPLICIT REAL*8(A-H,L-Z)
       DIMENSION X(6),XDOT(6)
C
       XDOT(1)=X(4)*SIN(X(5))
```

```
      XDOT(2)=X(4)*COS(X(5))*COS(X(6))/(X(1)*COS(X(3)))
      XDOT(3)=X(4)*COS(X(5))*SIN(X(6))/X(1)
      XDOT(4)=AS-G*SIN(X(5))
      XDOT(5)=(AR-G*COS(X(5))+X(4)*X(4)*COS(X(5))/X(1))/X(4)
      DUM=TAN(X(3))/X(1)
      XDOT(6)=AW/(COS(X(5))*X(4))-X(4)*COS(X(5))*COS(X(6))*DUM
C
      RETURN
      END
C
CCCCCCCCCCCCCCCCCCCCCCCCCCCCCCCCCCCCCCCCCCCCCCCCCCCCCCCCCCCCCCCCCCCCCCCCCC
C
C     THIS SUBROUTINE TAKES CARE OF ALL HARDCOPY OUTPUT
C
CCCCCCCCCCCCCCCCCCCCCCCCCCCCCCCCCCCCCCCCCCCCCCCCCCCCCCCCCCCCCCCCCCCCCCCCCC
C
      SUBROUTINE WRT(X,T,THR,MASS,ALPHA,AOB,RHO,N,M)
      IMPLICIT REAL*8(A-H,L-Z)
      DIMENSION X(6),XDOT(6)

      PI=3.14159265359D+0

      RADIUS=X(1)/1000.
      VELOCITY=X(4)/1000.
      GAMMA=X(5)*180./PI
      ALFA=ALPHA*180./PI
      HEAT=RHO**N*X(4)**M*9.652D-5
      SIGMA=AOB*180./PI
      OINC=ACOSD(COS(X(3))*COS(X(6)))
      DELTA=0.0
      IF (OINC .NE. 0.) DELTA=ASIND(TAN(X(3))/TAND(OINC))
      OMEGA=X(2)*180./PI-DELTA

      WRITE(13,1)T,RADIUS,VELOCITY,MASS,GAMMA,OINC,THR,HEAT,
     *ALFA,SIGMA

1     FORMAT(1X,F6.1,1X,F8.3,1X,F6.4,2X,F7.2,1X,F5.3,1X,
    * F6.3,1X,F7.1,1X,E9.3,1X,F7.3,1X,F7.3)
C
      RETURN
      END
C
CCCCCCCCCCCCCCCCCCCCCCCCCCCCCCCCCCCCCCCCCCCCCCCCCCCCCCCCCCCCCCCCCCCCCCCCCC
C
C     THIS SUBROUTINE ATTACH A HEADER TO THE OUTPUTS TO KEEP TRACK
C      OF THE DIFFERENT CHANGES
C
CCCCCCCCCCCCCCCCCCCCCCCCCCCCCCCCCCCCCCCCCCCCCCCCCCCCCCCCCCCCCCCCCCCCCCCCCC
C
      SUBROUTINE HDR(R,V,MASS,THR,VEC,GAMMA)
      IMPLICIT REAL*8(A-H,L-Z)
```

```
      DO 1 I=13,14
      IF (I.EQ.14)GO TO 1
      WRITE(I,*)
      WRITE(I,*)'  SELECTED INITIAL INPUT DATA:'
      WRITE(I,*)
      WRITE(I,2)R,V,MASS,THR,VEC,GAMMA
      WRITE(I,*)
      WRITE(I,*)
1     CONTINUE
2     FORMAT(' INITIAL RADIUS    (METERS)       ',F10.2,/,' INITIAL

     *VELOCITY  (METERS/SEC)      ',F7.2,/,' INITIAL MASS      (KG)
     *              ',F7.2,/,' INITIAL THRUST    (NEWTONS)       '
     *,F9.2,/,' THRUST VECTOR ANGLE (DEG)            '
     *,F6.2,/,' INITIAL FLIGHT PATH ANGLE (RADS)      ',F5.2)
C
      WRITE(13,*)'  TIME  RADIUS VELOCITY  MASS   GAMMA  INCLI
     * THRUST    QDOT     ALPHA    AOB'
      WRITE(13,*)' (SEC)   (KM)  (KM/SEC)  (KG)   (DEG)  (DEG)
     *   (N)    (J/M2S)   (DEG)   (DEG)'
C
      RETURN
      END
C
CCCCCCCCCCCCCCCCCCCCCCCCCCCCCCCCCCCCCCCCCCCCCCCCCCCCCCCCCCCCCCCCCCCCCCCCCC
C
C      THIS SUBROUTINE IS A FOURTH ORDER RUNGE-KUTTA ROUTINE TAKEN
C      FROM PROF. ROSS'S SUBROUTINE.
C
CCCCCCCCCCCCCCCCCCCCCCCCCCCCCCCCCCCCCCCCCCCCCCCCCCCCCCCCCCCCCCCCCCCCCCCCCC
C
      SUBROUTINE RK4(T,X,XDOT,NE,H,INDEX)
      IMPLICIT REAL*8(A-H,L-Z)
      INTEGER INDEX,I
      DIMENSION X(6),XDOT(6),SAVED(6),SAVEX(6)
C
      INDEX=INDEX+1
      GO TO (1,2,3,4),INDEX
1     DO 10 I=1,NE
      SAVEX(I)=X(I)
      SAVED(I)=XDOT(I)
10    X(I)=SAVEX(I)+.5D0*H*XDOT(I)
      T=T+.5D0*H
      RETURN
C
2     DO 20 I=1,NE
      SAVED(I)=SAVED(I)+2.D0*XDOT(I)
20    X(I)=SAVEX(I)+.5D0*H*XDOT(I)
      RETURN
C
3     DO 30 I=1,NE
```

```
      SAVED(I)=SAVED(I)+2.D0*XDOT(I)
30    X(I)=SAVEX(I)+H*XDOT(I)
      T=T+.5D0*H
      RETURN
C
4     DO 40 I=1,NE
40    X(I)=SAVEX(I)+H/6.D0*(SAVED(I)+XDOT(I))
      INDEX=0
      RETURN
      END
```

SAMPLE AERO.DAT INPUT FILE

This file gives the aerodynamic data used for the MRRV.

C1-6,AOPT,N,M,S,MASS,FM,SPI,THRUST

```
COEFFICENT C1        -1.000000D-02
COEFFICENT C2         2.860000D-01
COEFFICENT C3         1.313000D+00
COEFFICENT C4         4.700000D-02
COEFFICENT C5        -4.470000D-01
COEFFICENT C6         2.040000D+00
AOA FOR CL/CD MAX     1.823870D-01
AOB FOR BANG MANU     1.570796D+00
DENSITY EXPONENT      0.500000D+00
VELOCITY EXPONENT     3.150000D+00
REFERNCE AREA         1.169800D+01
INITIAL MASS (KG)     4.898000D+03
FINAL MASS   (KG)     4.800000D+03
SPECIFIC IMPULSE (S) 2.950000D+02
THRUST (N)            1.467900D+04
THRUST ANGLE (RAD)    0.261800D+00
```

SAMPLE DATA.DAT INPUT FILE

This file gives the orbital and time printing information for the simulation program.

INPUT ORBITAL PARAMETERS

```
RADIUS METERS        6.4450000D+06
THETA RADIANS        0.0000000D+00
PHI   RADIANS        0.0000000D+03
VELOCITY M/S         7.7100000D+03
FLIGHT PATH ANGLE    0.0000000D+00
PSI   RADIANS        0.0000000D+00
BEGIN TIME SEC       0.0000000D+00
END TIME SEC         4.0000000D+03
TIME INTERVAL SEC    5.0000000D-03
PRINT TIME INTERVAL 1.0000000D+00
```

SAMPLE OUT.DAT OUTPUT FILE

SELECTED INITIAL INPUT DATA:

NITIAL RADIUS	(METERS)	6445000.00
NITIAL VELOCITY	(METERS/SEC)	7710.00
NITIAL MASS	(KG)	4898.00
NITIAL THRUST	(NEWTONS)	14679.00
HRUST VECTOR ANGLE	(DEG)	15.00
NITIAL FLIGHT PATH ANGLE	(RADS)	0.00

TIME (SEC)	RADIUS (KM)	VELOCITY (KM/SEC)	MASS (KG)	GAMMA (DEG)	INCLI (DEG)	THRUST (N)	QDOT (J/M2S)	ALPHA (DEG)	AOB (DEG)
0.0	6445.000	7.7100	4898.00	0.000	0.000	14679.0	0.147E+07	30.615	90.000
1.0	6445.000	7.7100	4892.95	-.003	0.037	14679.0	0.147E+07	30.937	90.000
2.0	6444.999	7.7099	4887.88	-.006	0.074	14679.0	0.147E+07	31.254	90.000
3.0	6444.998	7.7097	4882.80	-.008	0.112	14679.0	0.147E+07	31.567	90.000
4.0	6444.997	7.7095	4877.73	-.011	0.150	14679.0	0.147E+07	31.876	90.000
5.0	6444.995	7.7092	4872.65	-.014	0.189	14679.0	0.147E+07	32.181	90.000
6.0	6444.993	7.7088	4867.58	-.017	0.228	14679.0	0.147E+07	32.482	90.000
7.0	6444.991	7.7084	4862.50	-.019	0.268	14679.0	0.147E+07	32.779	90.000
8.0	6444.988	7.7079	4857.43	-.022	0.309	14679.0	0.147E+07	33.074	90.000
9.0	6444.985	7.7074	4852.36	-.025	0.349	14679.0	0.147E+07	33.365	90.000
10.0	6444.981	7.7068	4847.28	-.028	0.391	14679.0	0.147E+07	33.653	90.000
11.0	6444.977	7.7061	4842.21	-.031	0.433	14679.0	0.147E+07	33.938	90.000
12.0	6444.973	7.7053	4837.13	-.034	0.475	14679.0	0.147E+07	34.221	90.000
13.0	6444.968	7.7045	4832.06	-.036	0.518	14679.0	0.147E+07	34.501	90.000
14.0	6444.963	7.7037	4826.98	-.039	0.561	14679.0	0.147E+07	34.778	90.000
15.0	6444.958	7.7027	4821.91	-.042	0.605	14679.0	0.147E+07	35.054	90.000
16.0	6444.952	7.7017	4816.84	-.045	0.649	14679.0	0.147E+07	35.327	90.000
17.0	6444.946	7.7006	4811.76	-.048	0.694	14679.0	0.147E+07	35.598	90.000
18.0	6444.939	7.6995	4806.69	-.051	0.739	14679.0	0.147E+07	35.868	90.000
19.0	6444.932	7.6983	4801.61	-.054	0.785	14679.0	0.147E+07	36.135	90.000
19.3	6444.930	7.6979	4799.99	-.055	0.800	14679.0	0.147E+07	36.219	90.000

LIST OF REFERENCES

1. Walberg, Gerald D., "A Survey of Aeroassisted Orbit Transfer," *Journal of Spacecraft and Rocket*, v. 22, January-February 1985.

2. Mease, Kenneth D., Lee, J.Y., and Vinh, N.X., "Orbital Changes During Hypersonic Aerocruise", *The Journal of the Astronautical Sciences*, v. 36, January-February 1988.

3. Spriesterbach, Thomas P., *Performance Analysis of Non-Coplanar Synergetic Maneuvers*, Master's Thesis, Naval Postgraduate School, Monterey, California, December 1991.

4. Ikawa, Hideo and Rudiger, Thomas F., "Synergetic Maneuvering of Winged Spacecraft for Orbital Plane Change," *Journal of Spacecraft and Rocket*, v. 19, November-December 1982.

5. Mease, Kenneth D. and Utashima, Masayoshi, "Effect of Heat Rate Constraint on Minimum-Fuel Synergetic Plane Change", paper presented at the AAS/AIAA Spaceflight Mechanics Meeting, Houston, Texas, 11-13 February 1991.

INITIAL DISTRIBUTION LIST

		No. Copies
1.	Defense Technical Information Center Cameron Station Alexandria VA 22304-6145	2
2.	Library, Code 052 Naval Postgraduate School Monterey CA 93943-5002	2
3.	Department Chairman, Code AA Department of Aeronautics and Astronautics Naval Postgraduate School Monterey, California 93943-5000	1
4.	Department of Aeronautics and Astronautics ATTN: Professor I.M. Ross, Code AA/Ro Naval Postgraduate School Monterey, California 93943-5000	7
5.	Department of Aeronautics and Astronautics ATTN: Professor Raymond P. Shreeve, Code AA/Sf Naval Postgraduate School Monterey, California 93943-5000	1
6.	LT Richard E. Johnson, USN 4819 Station House Lane Virginia Beach, Virginia 23455	2